Available online at www.sciencedirect.com
SCIENCE DIRECT®
Journal of Sound and Vibration 283 (2005) 401–432
JOURNAL OF SOUND AND VIBRATION
www.elsevier.com/locate/jsvi

Hydrofoil vibration induced by a random flow: a stochastic perturbation approach

Antonio Carcaterra[a,*], Daniele Dessi[b], Franco Mastroddi[c]

[a]*Dipartimento di Meccanica e Aeronautica, Università di Roma, 'La Sapienza', Via Eudossiana, 18, 00184 Rome, Italy*
[b]*INSEAN, Istituto Nazionale per Studi ed Esperienze di Architettura Navale, Via di Vallerano, 139, 00128 Rome, Italy*
[c]*Dipartimento di Ingegneria Aerospaziale e Astronautica, Università di Roma, 'La Sapienza', Via Eudossiana, 18, 00184 Rome, Italy*

Received 5 August 2002; received in revised form 20 April 2004; accepted 21 April 2004
Available online 14 November 2004

Abstract

The problem of an elastic lifting hydrofoil in a randomly perturbed flow is considered. It appears that in these conditions the phenomenon of hydroelastic-induced vibrations is controlled by a stochastic differential operator. By using the theory of stochastic perturbation, a technique of solution for this class of problems is proposed, leading to an effective numerical solution. The fundamentals of the method are given and it is applied to the general problem of hydroelastic vibrations. A numerical application to the case of an elastic control surface for a prototype-high- speed marine vehicle is presented. Comparisons between the results obtained by the Stochastic Perturbation Method (SPM) and those provided by standard Monte Carlo simulations (MCS) show the accuracy of the proposed method and a useful saving in computational time. A method is given for comparing the computational time required by the two methods, for a given statistical accuracy.

1. Introduction

This paper is focused on flow-induced vibrations of an elastic hydrofoil in a randomly perturbed flow: stochastic fluctuations of the inflow velocity are superimposed to an average

*Corresponding author. Tel.: +39-06-445-85-794; fax: +39-06-484-654.
E-mail address: a.carcaterra@dma.ing.uniroma1.it (A. Carcaterra).

0022-460X/$ - see front matter © 2004 Elsevier Ltd. All rights reserved.
doi:10.1016/j.jsv.2004.04.040

deterministic flow component. The problem, per se theoretically interesting, is not of small practical importance. In fact, it arises at the design stage of marine or aerospace engineering. A typical case is represented by the control surfaces of high-speed vessels, such as rudders and stabilization fins, especially when a fatigue life estimate of the structural component is required.

Whatever the model used to represent the coupled fluid–structure response, a direct numerical solution of the problem presents some troubles. In fact, a random perturbation of the inflow velocity makes stochastic the differential operator governing the coupled fluid-structural motion. This means that a single direct numerical integration of such a system provides just one sample of a stochastic process, so that the single-case simulation has not any statistical meaning. Thus, a significant solution of the problem can be achieved only in probabilistic terms. A way to handle these problems is via the Monte Carlo simulation. However, it is known that this technique is very time consuming [1–3]. Moreover, a post-processing of the results is needed to provide the relevant statistical data, such as the mean and the standard deviation of the response.

Several other methods can be used to deal with stochastic response of a linear or nonlinear systems [4–7]. A short review of some of them is given in the following section.

The basic idea developed in this paper is to approach the problem via a Stochastic Perturbation Method (SPM) [2,4] together with the Rice decomposition [8] when solving the hydroelastic equation of motion. The method is applied to a problem of hydroelasticity consisting of an elastic surface undergoing a random flow. The formulation of this problem leads to a set of linear differential equations with time-dependent stochastic coefficients. The solution, in terms of Lagrangian variables associated with hydroelastic vibrations is provided directly in terms of the sought after statistical moments up to the second order.

A systematical comparison with the numerical results obtained by a direct Monte Carlo simulation, performed on a very large number of realizations, shows the reliability of the proposed stochastic perturbation technique that keeps the relevant statistics of the phenomenon at a low computational cost.

This method seems to be effective and innovative, considering that while SPM has its established formulation in the theory of stochastic differential equations, it has not yet its firm position as an engineering tool in the frame of fluid–structure interaction. The case here analyzed of hydroelastic problem is particularly relevant, since, as it will be clear in Section 3, a randomly perturbed flow about an elastic body leads to prototype stochastic equations of the form given in Section 2, for which SPM has good chances. Moreover, as far the authors know, this method has never been considered for the solution of fluid–structure interaction problems.

2. Stochastic differential operators and perturbation techniques

Consider a physical system controlled by the general differential equation:

$$L(\mathbf{u}, \mathbf{Du}, \mathbf{P}) = f(\mathbf{x}, t) \tag{1}$$

being a linear or a nonlinear form L of the arguments $\mathbf{u}$, $\mathbf{Du}$ and $\mathbf{P}$; $\mathbf{u}(\mathbf{x},t)$ is the field descriptor depending, in general, on the space and time coordinates $\mathbf{x}$ and t, $\mathbf{Du}$ is a vector containing partial derivatives of $\mathbf{u}(\mathbf{x},t)$, with respect to $\mathbf{x}$ and t up to an arbitrary order, and $\mathbf{P}$ is a vector of coefficients accounting for some field properties. Finally, $f(\mathbf{x},t)$ is the external input to the

considered system. Eventually, boundary and initial conditions complete the problem posed by Eq. (1).

In the frame of the analysis of physical systems involving a random process, different cases should be distinguished [4,6], having the corresponding problems a deeply different nature. A random process can actually affect $f(\mathbf{x},t)$, $\mathbf{P}$ or even the boundary and initial conditions related to Eq. (1) (however, this last case is not of interest for the subject of the present paper).

Consider the case in which $f(\mathbf{x},t)$ is a random function, while $\mathbf{P}$ is a vector of deterministic properties. Assume in addition that L is linear with respect to $\mathbf{u}$.

This configuration belongs to the classical theory of linear systems with a random stationary input: provided that the statistics of $f(\mathbf{x},t)$ is known, generally by its auto-correlation function R_{ff} (or by its spectral density), let us determine the statistics of the output field descriptor $\mathbf{u}(\mathbf{x},t)$, e.g. providing its auto-correlation function R_{uu} (or its spectral density). This is the more widespread statement of random vibration problems in engineering, for which well-known formulations are available in the frame of a general theory since a long time [3,4,9] and are well established also in engineering analysis of practical systems. In aeroelasticity, the aircraft elastic response to a stochastic gust profile [10–12] belongs to this class of problems and the solution, provided in terms of power spectral density, is widely used both at design stage and to meet the requirements imposed by aircraft authority.

In the previously mentioned problems, the random process only affects the external input force $f(\mathbf{x},t)$, while the system exhibits per se (i.e., the operator L) a deterministic behavior.

However, more general statements of the random vibration problem are met in the analysis of engineering systems. Indeed, in some cases, the nature of the studied system presents a random uncertainty, e.g., its geometric and mechanical characteristics or, as in the present paper, its interaction with a surrounding fluid in random motion. In this case, besides f, $\mathbf{P}$ is also stochastic, making the operator L itself stochastic. These problems led naturally to consider a stochastic population of samples having stochastic properties. If the sample we are considering is a system described via Eq. (1), then a random population of samples is obtained when randomly varying the parameter $\mathbf{P}$. In correspondence, a random population of solutions $\mathbf{u}(\mathbf{x},t)$ is also determined. Thus, a second class of random problems is formulated as follows: assuming the probability of the property vector $\mathbf{P}$, provide the probability of the solution $\mathbf{u}(\mathbf{x},t)$.

A direct answer to the last problem is provided by the Monte Carlo method [2,3]. It consists of solving a population of equations of form (1) by randomly varying $\mathbf{P}$. Each of the considered problem is completely deterministic and it is solved by using a standard algorithm (analytical or numerical). As a result, a random population of solutions is obtained and a statistics is performed on it. The advantage of such a technique relies on the theoretical simplicity and generality of the method, since no special hypotheses neither about the linearity of L nor about the properties of the random process are needed. On the other hand, this obviously implies a heavy numerical burden. In fact, a significant statistics can be performed only when a large enough number of solution samples are generated, i.e., only when Eq. (1) is solved many times with different sample values of $\mathbf{P}$. The theory of probability [3,13] provides directions concerning the number of samples to employ in order to get a significant statistics but, in general, this number is large.

The analysis of stochastic problems, whatever the nature of the operator L (linear or nonlinear) and whatever the nature of the considered randomness, $\mathbf{P}$ and/or f, is dealt in a general way by the

Fokker–Plank–Kolmogorov (FPK) equations [3,4,6], providing a functional equation relating the probability density functions of the stochastic processes, i.e., of $\mathbf{P}$ and f, to that of the solution $\mathbf{u}$. Unfortunately, the formal complexity of this partial differential equations induces, in many cases, to skip this approach.

The complexity of the FPK equations is highly reduced if the desired information is limited to the statistical moments of the solution $\mathbf{u}$. A suitable application of the expectation operator (average operator) to both sides of the FPK equations leads to a set of first-order ordinary differential equations in terms of statistical moments of the solution (moment equations). Early introduction of this approach is that of Bogdanof and Kozin [14] and of Cumming [15]. This averaging technique is a powerful tool in dealing with stochastic operators and inspires many methods of solutions of stochastic differential equations [4,16,17]. In a sense, the method of weighted residuals [2,6,18], that is also the basis of many general solution techniques, can be also derived from the same idea. A well known and effective representative of the method of weighted residual is statistical linearization [19], that applies to L nonlinear and a random input f: an equivalent linear form $L_e(\mathbf{u}, \mathbf{Du}, \mathbf{P}_e) = f(\mathbf{x}, t)$ replaces the original nonlinear equation, where $\mathbf{P}_e$ is determined by satisfying the requirement of minimizing the standard deviation of the equation error (i.e., of a weighted residual). In this way, the problem is turned again to the theory of linear systems with random input.

The method of weighted residuals originates also the polynomial chaos technique that, since the early work of Wiener [20], is today a well-established tool in the solution of stochastic differential problems [2,18]. Recently, Ghanem and Spanos disclosed unambiguously the subject into the field of engineering with the introduction of a spectral-based stochastic finite element technique [2]. Very recent and interesting application of this technique to fluid and fluid–structure interaction problems are presented in Refs. [21,22].

Polynomial chaos is based on the expansion of the stochastic process (f and/or $\mathbf{P}$) by using a suitable orthogonal polynomial basis with respect to the weighting function W (Hermite, Laguerre, Jacobi etc.) containing stochastic parameters (random events responsible for the system uncertainty). The solution $\mathbf{u}$ is also projected on the polynomial basis and the generalized Fourier coefficients are the deterministic unknowns of the problem. Direct application of the Galerkin method provides the desired solution: $\mathbf{u}$, f and/or $\mathbf{P}$ spanned on the polynomial basis are substituted into Eq. (1) that is projected onto each polynomial of the chosen basis, imposing that the equation error for each equals zero. Since the polynomials contain the randomness, the weighting function W can be viewed as the probability density function (pdf) of the random process, and the Galerkin procedure (weighted residuals) as a stochastic averaging of Eq. (1). Further features of this approach are discussed later in this section when discussing the canonical decomposition of a random process.

A different approach is provided indeed by the stochastic perturbation method (SPM). It was born in the frame of the theory of stochastic differential equations [2,4,23,24] with random coefficients as the natural generalization of the perturbation techniques used in deterministic nonlinear problems (see e.g., Ref. [25]). Although this approach is promising in the field of analysis considered in this paper, it has not yet received any particular attention to deal with random fluid-structure interaction problems. SPM uses the same scheme of perturbation techniques, although revisited in a stochastic light. The fundamentals of the theory and the approach followed in this paper are summarized below.

Analogously to other approaches to stochastic differential equations, the solution process here presented needs two basic elements: a suitable representation of the random process and a solution technique of the equations in which this random process is involved.

The analysis starts with the first step, expressing the properties vector $\mathbf{P}$ by the decomposition:

$$\mathbf{P} = \mathbf{P}_0(1+\varepsilon) = \mathbf{P}_0 + \tilde{\mathbf{P}}, \tag{2}$$

where $\mathbf{P}_0$ is a deterministic vector and ε is a small random perturbation whose expected value is $E\{\varepsilon\} = 0$ and the standard deviation is $E\{\varepsilon^2\} = \sigma_\varepsilon^2$. In Eq. (2) and in the rest of the paper, the terms with symbol tilde like $\tilde{\mathbf{P}}$ denote random variables. The posed problem consists of determining the mean and the standard deviation of $\mathbf{u}(\mathbf{x},t)$ as a function of the input data statistics, e.g., σ_ε^2. For the sake of simplicity, the notation $\mathbf{\Psi} = (\mathbf{u}, \mathbf{Du})^{\mathrm{T}}$ is introduced. The second step assumes the solution by the following stochastic expansion:

$$\mathbf{\Psi} = \mathbf{\Psi}_0 + \varepsilon\mathbf{\Psi}_1 + \varepsilon^2\mathbf{\Psi}_2 + o(\varepsilon^2) = \mathbf{\Psi}_0 + \tilde{\mathbf{\Psi}}, \tag{3}$$

where $\mathbf{\Psi}_0, \mathbf{\Psi}_1, \mathbf{\Psi}_2$ are deterministic vectors, while $\mathbf{\Psi}$ is the wished random solution. By performing a Taylor series expansion (up to the second order) of L around $\mathbf{\Psi}_0$, $\mathbf{P}_0$ and by substituting Eqs. (2) and (3) into Eq. (1), it yields

$$\begin{aligned} L(\mathbf{\Psi},\mathbf{P}) = {} & L(\mathbf{\Psi}_0,\mathbf{P}_0) + \mathbf{L}_\Psi^{\mathrm{T}}(\mathbf{\Psi}_0,\mathbf{P}_0)\tilde{\mathbf{\Psi}} + \mathbf{L}_P^{\mathrm{T}}(\mathbf{\Psi}_0,\mathbf{P}_0)\tilde{\mathbf{P}} + \tilde{\mathbf{\Psi}}^{\mathrm{T}}\mathbf{L}_{\Psi\Psi}(\mathbf{\Psi}_0,\mathbf{P}_0)\tilde{\mathbf{\Psi}} + \tilde{\mathbf{P}}^{\mathrm{T}}\mathbf{L}_{PP}(\mathbf{\Psi}_0,\mathbf{P}_0)\tilde{\mathbf{P}} \\ & + \tilde{\mathbf{\Psi}}^{\mathrm{T}}\mathbf{L}_{\Psi P}(\mathbf{\Psi}_0,\mathbf{P}_0)\tilde{\mathbf{P}} + \tilde{\mathbf{P}}^{\mathrm{T}}\mathbf{L}_{P\Psi}(\mathbf{\Psi}_0,\mathbf{P}_0)\tilde{\mathbf{\Psi}}, \end{aligned}$$

where $\mathbf{L}_\Psi$, $\mathbf{L}_P$ are vectors of first-order derivatives, while $\mathbf{L}_{\Psi\Psi}$, $\mathbf{L}_{PP}$, $\mathbf{L}_{P\Psi}$, $\mathbf{L}_{\Psi P}$ are matrices of second-order derivatives of L. By expressing the dependency on ε and ordering with respect to its increasing powers, Eq. (1) leads to the cascade system of equations:

$$\begin{gathered} L(\mathbf{\Psi}_0,\mathbf{P}_0) = f(\mathbf{x},t), \\ \mathbf{L}_\Psi^{\mathrm{T}}(\mathbf{\Psi}_0,\mathbf{P}_0)\mathbf{\Psi}_1 + \mathbf{L}_P^{\mathrm{T}}(\mathbf{\Psi}_0,\mathbf{P}_0)\mathbf{P}_0 = 0, \\ \mathbf{L}_\Psi^{\mathrm{T}}(\mathbf{\Psi}_0,\mathbf{P}_0)\mathbf{\Psi}_2 + \mathbf{\Psi}_1^{\mathrm{T}}\mathbf{L}_{\Psi\Psi}(\mathbf{\Psi}_0,\mathbf{P}_0)\mathbf{\Psi}_1 + \mathbf{P}_0^{\mathrm{T}}\mathbf{L}_{PP}(\mathbf{\Psi}_0,\mathbf{P}_0)\mathbf{P}_0 \\ + \mathbf{\Psi}_1^{\mathrm{T}}\mathbf{L}_{\Psi P}(\mathbf{\Psi}_0,\mathbf{P}_0)\mathbf{P}_0 + \mathbf{P}_0^{\mathrm{T}}\mathbf{L}_{P\Psi}(\mathbf{\Psi}_0,\mathbf{P}_0)\mathbf{\Psi}_1 = 0. \end{gathered}$$

This system is deterministic and provides the three unknowns $\mathbf{\Psi}_0, \mathbf{\Psi}_1, \mathbf{\Psi}_2$. The statistics of $\mathbf{\Psi}$ is simply determined by applying the expected value operator $E\{\cdot\}$ to expression (3):

$$E\{\mathbf{\Psi}\} = \mathbf{\Psi}_0 + \sigma_\varepsilon^2\mathbf{\Psi}_2. \tag{4}$$

Moreover, the correlation matrix is

$$E\{\mathbf{\Psi}\mathbf{\Psi}^{\mathrm{T}}\} = \mathbf{\Psi}_0\mathbf{\Psi}_0^{\mathrm{T}} + \sigma_\varepsilon^2[\mathbf{\Psi}_0\mathbf{\Psi}_2^{\mathrm{T}} + \mathbf{\Psi}_1\mathbf{\Psi}_1^{\mathrm{T}} + \mathbf{\Psi}_2\mathbf{\Psi}_0^{\mathrm{T}}]. \tag{5}$$

These equations provide the desired result: the statistics of the solution is given in terms of the statistics of the data.

A more complex situation arises when the vector of the properties $\mathbf{P}$ is a stochastic function and not a simple random variable. This implies that $\mathbf{P}(\mathbf{x},t)$ depends on the independent variables $(\mathbf{x},t)$, representing field properties randomly varying in space and time. This case can be substantially reduced to the previous one when a canonical decomposition is used. This concept leads to a reconsideration of classical projection methods (e.g. that of Galerkin) from a stochastic point of view. By introducing a set of linearly independent functions $\mathbf{\Pi}(\mathbf{x},t)$ in R^4, then $\mathbf{P}(\mathbf{x},t)$ can be

expressed as

$$\mathbf{P}(\mathbf{x},t) = \mathbf{P}_0(\mathbf{x},t) + \mathbf{\Gamma\Pi}(\mathbf{x},t), \tag{6}$$

where $\mathbf{\Gamma}$ is a matrix containing generalized Fourier coefficients. When $\mathbf{P}(\mathbf{x},t)$ represents a random process, it can be thought that the decomposition (6) can be operated for each observed sample of the population of functions $\mathbf{P}(\mathbf{x},t)$.

This approach was introduced since 1945 by Rice [8] in the analysis of random noise currents of electric devices. In this case $\mathbf{\Pi}(\mathbf{x},t)$ are harmonic functions and expansion (6) results in a Fourier series.

Moreover, the randomness of $\mathbf{P}(\mathbf{x},t)$ implies that, for any observed sample, the associated Fourier coefficients have different values. Thus, the Rice's decomposition (6) is legitimate provided that $\mathbf{\Gamma}$ is a matrix of random coefficients. In this way $\mathbf{P}(\mathbf{x},t)$ is collapsed into the set of simple random variables Γ_{ij}. Therefore it is apparent how expression (2) is just a special (and simpler) case of expression (6) (obtained for $\mathbf{\Gamma} \equiv \varepsilon\mathbf{P_0}$ and $\mathbf{\Pi} \equiv 1$). Decomposition (4) is said canonical if $E\{\Gamma_{ij}\} = 0$ and $E\{\Gamma_{ij}\Gamma_{rs}\} = \delta_{ir}\delta_{js}\sigma^2_{\Gamma_{ij}}$. Rice's decomposition (6) can describe both stationary and unsteady random processes and is used in this paper to describe the random inflow as shown later.

It is worth to be noted that expansion (6) also presents a formal similarity to the polynomial chaos expansion [2,18,20]. However, in the theory of polynomial chaos the roles of $\mathbf{\Pi}(\mathbf{x},t)$ and $\mathbf{\Gamma}$ are reversed with respect to the Rice's decomposition: $\mathbf{\Pi}(\mathbf{x},t)$ represents a set of orthogonal polynomials containing the uncertainty in terms of a random event, while $\mathbf{\Gamma}$ are deterministic coefficients.

Once the Rice's decomposition of $\mathbf{P}(\mathbf{x},t)$ is performed, a generalized Taylor expansion of the solution $\mathbf{\Psi}$ in correspondence of the expected value $E\{\Gamma_{ij}\}$ in terms of $\mathbf{\Gamma}$ can be introduced:

$$\Psi_i = \Psi_{0i} + \sum_{rs} \frac{\partial \Psi_i}{\partial \Gamma_{rs}} \Gamma_{rs} + \sum_{r\,s\,h\,k} \frac{\partial^2 \Psi_i}{\partial \Gamma_{rs} \partial \Gamma_{hk}} \Gamma_{rs}\Gamma_{hk} + \cdots$$

or

$$\mathbf{\Psi} = \mathbf{\Psi}_0 + \mathbf{\Psi}_1\mathbf{\Gamma} + \mathbf{\Gamma}^{\mathrm{T}}\mathbf{\Psi}_2\mathbf{\Gamma} + o\left(\mathbf{\Gamma}^{\mathrm{T}}\mathbf{\Gamma}\right).$$

In these equations, the deterministic unknowns are $\mathbf{\Psi}_1$ and $\mathbf{\Psi}_2$, while the statistics of the coefficients Γ_{ij} is given. The procedure is analogous to that followed starting from Eq. (2) through Eqs. (5) and (6).

The main features of the stochastic perturbation method here considered can be summarized as follows: (i) the stochastic process $\mathbf{P}$ is expressed by a harmonic stochastic series (Rice), each term being the product of a deterministic function $\mathbf{\Pi}(\mathbf{x},t)$ (sine and cosine basis) times random Fourier coefficients $\mathbf{\Gamma}$, (ii) the solution $\mathbf{u}$ is expressed by a Taylor series of Fourier coefficients $\mathbf{\Gamma}$ of the Rice's decomposition, (iii) the unknowns are the Taylor's series coefficients, (iv) any randomness in the final equations (deterministic) is canceled out due to the power ordering.

Analogies and differences with respect to the polynomial chaos approach are apparent considering the following characteristic of polynomial chaos: (i) the stochastic process is expressed by the polynomial chaos, each term being the product of a deterministic function $\mathbf{\Gamma}$ (generalized Fourier coefficients) times a stochastic polynomial basis $\mathbf{\Pi}(\mathbf{x},t)$ (roles of $\mathbf{\Pi}(\mathbf{x},t)$ and $\mathbf{\Gamma}$ are reversed), (ii) both the solution $\mathbf{u}$ and the process $\mathbf{P}$ are spanned over the same

orthogonal basis, (iii) the unknowns are the generalized Fourier coefficients $\mathbf{\Gamma}$, and (iv) any randomness in the final equations (deterministic) is canceled out due to the use of orthogonality relationships.

Thus, both in the polynomial chaos technique and in the SPM method, based on the Rice's decomposition, the random process is expanded onto a rich basis containing, in general, many terms. However, the main advantage offered by the SPM relies on a simpler expansion of the solution that, as in the present paper, is considered only up to the second order, while the polynomial chaos expansion uses again a larger number of terms (i.e. the same basis used for the random process expansion). The counterpart of this advantage is that polynomial chaos is in general more accurate and is more flexible since, by a suitable choice of the polynomial basis [2,18], a large number of different probabilistic distributions of the random process $\mathbf{P}$ can be considered, being the Rice's decomposition suitable to describe Gaussian processes only.

In the following sections an elastically suspended hydrofoil in a random flow is considered leading to a state-space model (see Section 3.1 and Appendix A for details):

$$\dot{\mathbf{y}} = \mathbf{A}(\mathbf{P})\mathbf{y} + \mathbf{b}(\mathbf{P}), \tag{7}$$

that is a special case of Eq. (1), where $\mathbf{y}$ is the state vector, $\mathbf{b}$ is the load vector and $\mathbf{A}$ is the aero/hydroelastic-system matrix. $\mathbf{P}$ depends on the inflow velocity parameters. Usually in standard aeroelasticity the effects of a random inflow are included in $\mathbf{b}$, e.g., this is the case of a vertical/lateral gust experienced by an aircraft, while the matrix $\mathbf{A}$ is assumed to be deterministic.

Indeed, in this case the perturbation velocity components are orthogonal to the undisturbed flow and this kind of perturbation (typically denoted as "downwash", see, e.g., Ref. [10]) is physically able to un-symmetrize the flow field physically modifying the shed vorticity at the trailing-edge and thus generating the unsteady aerodynamic forces: the theory of linearized potential flow gives a mathematical description of these phenomena—after a space discretization via, e.g., a panel method and after a reduction to a space-state format [26,27]—by the linear equation (7) with $\mathbf{A}$ independent by the perturbation $\mathbf{P}$ and $\mathbf{b}$ dependent as well.

However, in general, the matrix $\mathbf{A}$ exhibits a parametric dependency on the flow characteristics. This is, for instance, the case of head-on gust impinging upon an aircraft [5]. Thus, when a random inflow is considered, an additional randomness should be induced in the aero/hydroelastic matrix so that it also depends on the stochastic process $\mathbf{P}$. Indeed, in this case the perturbation involves only the flow-wise component of the velocity. Thus, the related aerodynamic forces are dependent on the state-space variables and the induced aerodynamic forces cannot be considered as an external (stochastic) input but only as a perturbation of the system parameters. On a physical point of view, this kind of perturbation would be unable to unsymmetrize the flow field and, therefore, to generate aerodynamic external loads. On the mathematical point of view, the system is modeled only by the portion $\dot{\mathbf{y}} = \mathbf{A}(\mathbf{P})\mathbf{y}$ of Eq. (7).

In conclusion of this section, while the randomness of $\mathbf{b}$ is included in the classical theory of random oscillations [3,9], the randomness of the operator $\mathbf{A}$ is not, and it can be dealt in the frame of SPM. For this reason, the following analysis is focused on the second mentioned case of randomness.

3. Statement of the stochastic hydroelastic problem and its SPM solution

The SPM outlined in the previous section is here applied to a specific problem: the prediction of the hydroelastic response of a submerged hydrofoil under a randomly fluctuating flow described by Eq. (7). The problem is modeled considering an elastic hydrofoil undergoing a chord-wise flow affected by a random velocity perturbation in the same direction of the main flow due to a surface traveling wave (see Figs. 1 and 2).

It is worth underlining that the load exerted on the structure by the fluid is supposed to be affected by the presence of the free-surface only through inflow velocity perturbations. On the other hand, the presence of the free-surface does not imply finite-domain effects on the flow field under suitable hypotheses that will be discussed in Section 3.1. This avoids the necessity to overly complicate the discussion of the SPM solution for the physical problem.

In Section 3.2 the coupled fluid–structure equations for 2D and 3D cases are introduced without no reference to the randomness of the velocity, which is related to the free-surface perturbations (waves) in Section 3.3. Thus, the hydroelastic equations depending on the randomly perturbed mean flow are suitable to be solved with the SPM as shown in Section 3.4. Finally, a comparison between SPM and MCS solutions in terms of computational efficiency is presented in Section 3.5 for the case of a prototype equation.

3.1. Remarks on free surface effects

In the present model, the origin of the inflow velocity perturbations is attributed to random waves generated on the water surface due to the wind action. These waves are described by the Airy theory [28], and the Pierson–Moskowitz [29] spectrum is assumed to statistically represent the wave surface elevation.

The waves traveling on the surface induce random velocity perturbations in the water depending on the depth. More precisely, the Airy waves theory [28] predicts an exponential decay

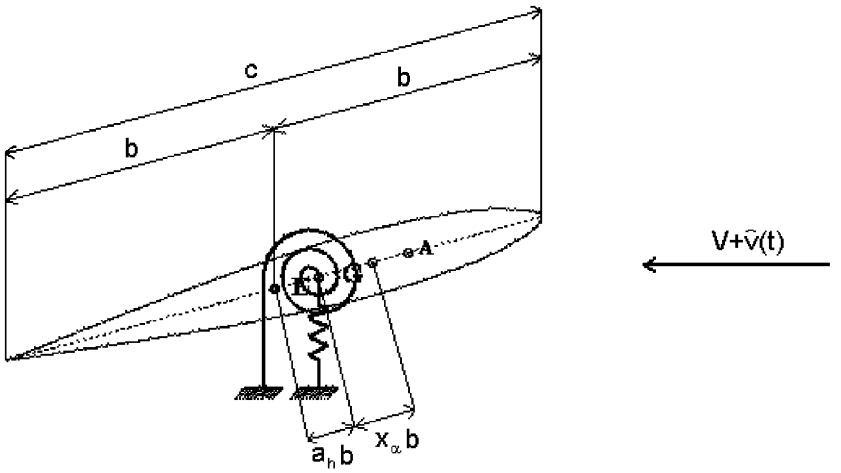

Fig. 1. Sketch of the typical-section model with stochastic inflow.

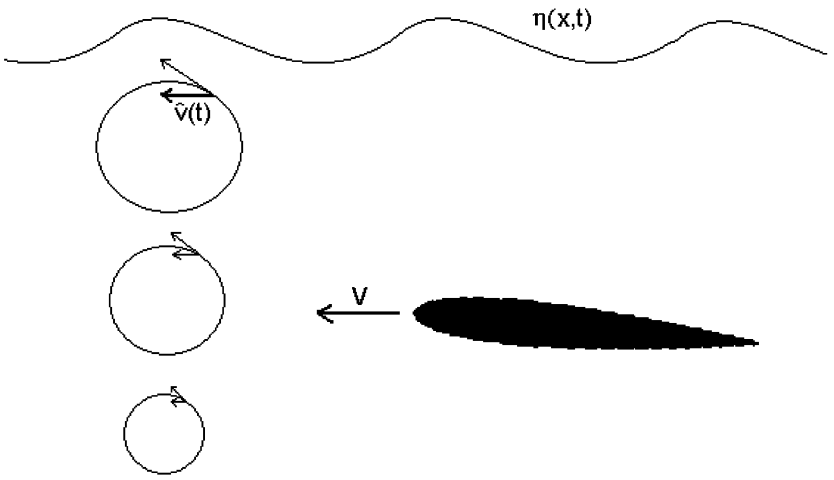

Fig. 2. Onset of the stochastic perturbation on the mean flow velocity due to traveling waves on the sea surface.

$e^{(2\pi/\lambda)z}$ of the disturbance, where λ is the wavelength on the water surface and z is the depth ($z=0$ at the near free surface, z positive downward). Thus, the disturbance is sensibly perceived if $h<\lambda$, where h is the considered depth of the hydrofoil.

The hydrofoil model considered in this paper is based on the hypothesis of linear, potential, attached, incompressible flow around a thin and planar lifting body in an infinite domain. However, this last hypothesis does not hold strictly in the considered physical problem because the free surface is present. Nevertheless, when the distance between the hydrofoil and the free surface is greater than about a chord length $2b$, lift perturbation effects, induced by the free surface on the hydrofoil, are reasonably negligible. This requirement is met when $h>2\,b\kappa$, where, following different authors [30], $\kappa \approx 1 \div 2$ is an acceptable value.

Therefore, it can be concluded that the model used here is physically consistent under the condition $\lambda > h > 2\,b\kappa$, implying that the hydrofoil depth is small enough to be affected by the wave random perturbations, but large enough to avoid the modeling of the free surface effects on the hydroelastic hydrofoil response.

With these assumptions we are in the position of developing a simple fluid–structure model dealing with the considered problem. Theodorsen's theory [31] for the 2D problem and lifting surface approach for the 3D one, are employed to achieve analytical and numerical solutions of the hydroelastic problem, respectively. These theories provide the generalized unsteady aerodynamic forces due to an arbitrary motion described in terms of Lagrangean variables. It is worthwhile to point out that the Theodorsen model, originally formulated in the frequency domain, can be transposed in terms of integral-differential equations in the time domain. Moreover these can be collapsed into a set of purely differential equations when using Finite-State aerodynamics (see Refs. [32,33] for details) so that the model assumes the form given by Eq. (7). In the same way, this approach has been considered in aeroelastic modeling for 3D hydroelastic applications presented in this paper [26,27].

3.2. The hydroelastic equations for a thin control-foil: 2D and 3D cases

The displacement field of a 3D elastic body can be generally expressed by the modal decomposition

$$\mathbf{u}(\mathbf{x},t)=\sum_{i=1}^{\infty}\mathbf{\Phi}_i(\mathbf{x})q_i(t), \tag{8}$$

where $\mathbf{\Phi}_i(\mathbf{x})$'s are eigenfunctions satisfying the prescribed homogeneous boundary conditions, and $q_i(t)$'s are the Lagrangean coordinates. A similar expansion, containing only two terms, also applies to a 2D elastically suspended rigid hydrofoil (typical section, [34]):

$$\mathbf{u}(\mathbf{x},t)\cong\mathbf{\Phi}_1q_1(t)+\mathbf{\Phi}_2q_2(t)=\mathbf{k}\,h_p(t)+\mathbf{k}(x-x_e)\alpha(t),$$

where $\mathbf{k}$ is the unit vector parallel to z, whereas $h_p(t)$, $\alpha(t)$ are the plunge and pitch Lagrangean variables, respectively. The x-axis is chord-wise axis (positive towards the trailing edge) and x_e is the co-ordinate of the center of rotation. The hydrofoil is studied in this way as a simple two-degree-of-freedom system, elastically constrained by a pair of translational and torsional equivalent linear springs, oscillating in plunge and pitch (Fig. 1).

By using standard notations (see Fig. 1), the non-dimensional plunge deflection at the elastic center is denoted by $\xi=h_p/b$, where b is half the chord. The elastic axis is located at a distance $a_h\,b$ from the mid-chord (a_h is the dimensionless distance, considered with respect to the half-cord length b, between the center of the hydrofoil and the elastic axis), while the mass center is located at a distance $x_\alpha b$ from the elastic axis. With these assumptions, the hydroelastic equations of the typical section are

$$\ddot{\xi}+x_\alpha\ddot{\alpha}+\Omega^2\xi=-p(\xi,\alpha),\quad (x_\alpha/r_\alpha^2)\ddot{\xi}+\ddot{\alpha}+\alpha=r(\xi,\alpha), \tag{9}$$

where 'dot' denotes the derivative with respect to $\tau=\omega_\alpha t$, $\Omega=\omega_\xi/\omega_\alpha$, being ω_ξ and ω_α the uncoupled natural frequencies of heave and pitch modes, respectively; $r_\alpha=\sqrt{J/mb^2}$ is the dimensionless radius of gyration about the elastic axis where m and J are the mass and the moment of inertia per unit length (with respect to the elastic center), respectively.

For an incompressible two-dimensional flow, the following hydrofoil expressions for the lift p and the pitching moment r, respectively, are found [33]:

$$\begin{aligned}p(\xi,\alpha)&=(\ddot{\xi}-a_h\ddot{\alpha}+U\dot{\alpha})/\mu+\frac{2}{\mu}U\int_0^\tau\varphi(\tau-\sigma)\dot{w}_{3/4}(\sigma)\mathrm{d}\sigma,\\ r(\xi,\alpha)&=[a_h(\ddot{\xi}-a_h\ddot{\alpha})-1/2U(1-a_h)\dot{\alpha}-1/8\ddot{\alpha}]/\mu r_\alpha^2\\&\quad+1/\mu r_\alpha^2(1+2a_h)U\int_0^\tau\varphi(\tau-\sigma)\dot{w}_{3/4}(\sigma)\mathrm{d}\sigma,\end{aligned}$$

where $\mu=\pi\rho b^2/m$ is the mass ratio, $w_{3/4}=\dot{\xi}-(1/2-a_h)\dot{\alpha}+U\alpha$ is the downwash, $\varphi(t)$ is the Wagner function [32], $U=V/b\omega_\alpha$ the dimensionless inflow velocity and V is the inflow velocity, oriented along the x-axis. In order to eliminate the integral term, obtaining a pure differential

problem, it is put

$$\chi(\tau) = \int_0^\tau \varphi(\tau - \sigma)\dot{w}_{3/4}(\sigma)\,\mathrm{d}\sigma,$$

where $\chi(\tau)$, the augmented state, represents the circulatory part of the lift, due to the wake. The Laplace transform of the previous equation is $\chi(s) = \varphi(s)sw_{3/4}(s)$, whereas the Jones' rational approximation in the Laplace domain is

$$\varphi(s) = 1/s - \hat{a}/(s + \hat{b}) - \hat{c}/(s + \hat{d})$$

with $\hat{a} = 0.165$, $\hat{b} = 0.0455$, $\hat{c} = 0.335$, $\hat{d} = 0.3$. After some algebraic manipulation, Eq. (9) is recast as a system of three polynomial equations in the Laplace domain (see Ref. [33, 35] for more details). Transforming back to time domain, a first-order linear differential equation of type (7) is determined:

$$\dot{\mathbf{y}} = \mathbf{A}(U)\mathbf{y}, \tag{10}$$

where $\mathbf{y} = \{\xi, \alpha, \chi, \dot{\xi}, \dot{\alpha}, \dot{\chi}\}^{\mathrm{T}}$ is the state vector, and the coefficients of $\mathbf{A}(U)$ depend on the inflow dimensionless velocity U [36,37].

Eq. (10) applies also to a three-dimensional flexible wing. By using Eq. (8), its response in this case is described by its first M natural modes.

Considering an integral, linear, unsteady, aero/hydrodynamic formulation for potential flow around a lifting thin body and replacing the three-dimensional body by a lifting mean surface surrounded by an infinite fluid domain, a model similar to that introduced above can be developed. This is performed, e.g., in MSC.NASTRAN code (the doublet-lattice method, implemented in the sequence solution SOL 145, [12]). By coupling the hydrodynamic problem with the elastic vibrations of the hydrofoil, it results in hydroelastic vibrations given in terms of M modal variables, collected in the state-space vector $\mathbf{q}(t)$. It is governed, in the Laplace domain, by the following equation:

$$\left(\mathbf{M}s^2 + \mathbf{K}\right)\hat{\mathbf{q}} = q_d\mathbf{Q}(s; V)\hat{\mathbf{q}}, \tag{11}$$

where $\mathbf{M}$ and $\mathbf{K}$ are suitable diagonal mass and stiffness matrices, $\hat{\mathbf{q}}$ is the Laplace transform of $\mathbf{q}$, q_d is the dynamic pressure, and $\mathbf{Q}$ is the generalized aerodynamic force matrix, depending on the Laplace variable s and on the inflow velocity V. Following a procedure similar to that applied above for the 2D hydrofoil, $\mathbf{Q}$ can be approximated with rational matrix polynomial with respect to the dimensionless Laplace variable $p = sb/V$ [26,27,32,33] as

$$\mathbf{Q}(p) = \mathbf{A}_0 + p\mathbf{A}_1 + p^2\mathbf{A}_2 + (p\mathbf{I} - \mathbf{P})^{-1}p\mathbf{R}, \tag{12}$$

where the matrices $\mathbf{A}_i$, $\mathbf{P}$ and $\mathbf{R}$ are obtained by a best-fitting procedure. It is worth to point out that the mathematical structure of this approximation is also related to a physical meaning. Indeed, the polynomial contribution given by $\mathbf{A}_0 + p\mathbf{A}_1 + p^2\mathbf{A}_2$ represents a low-frequency stiffness, damping, and mass behavior associated to the aerodynamic force whereas the term $(p\mathbf{I} - \mathbf{P})^{-1}p\mathbf{R}$ can be associated to a higher-frequency delay mechanism in the aerodynamic-load generation due to the presence of the wake [27]. When introducing $\hat{\mathbf{r}} = (p\mathbf{I} - \mathbf{P})^{-1}\mathbf{R}\hat{\mathbf{q}}$, combining Eqs. (11) and (12) and transforming back to time domain, one

obtains Eq. (10), where now

$$\mathbf{y} = \begin{pmatrix} \mathbf{q} \\ \dot{\mathbf{q}} \\ \mathbf{r} \end{pmatrix}, \quad \mathbf{A}(V) = \begin{bmatrix} 0 & \mathbf{I} & 0 \\ -\mathbf{M}_c^{-1}\mathbf{K}_c & -\mathbf{M}_c^{-1}\mathbf{D}_c & q_d\mathbf{M}_c^{-1} \\ \mathbf{PR}\,(V/b) & 0 & (V/b)\,\mathbf{P} \end{bmatrix}.$$

Note that $\mathbf{r}$, inverse Laplace transform of $\hat{\mathbf{r}}$, has a role similar to the function χ for the 2D case. Moreover

$$\mathbf{M}_c = \left(\mathbf{M} - q_d\mathbf{A}_2\, b^2/V^2\right), \quad \mathbf{D}_c = \left(-q_d\mathbf{A}_1 b/V\right), \quad \mathbf{K}_c = \left[\mathbf{K} - q_d(\mathbf{A}_0 + \mathbf{R})\right].$$

Therefore, under the specified physical assumptions, the hydroelastic vibration of the 3D system is described again by the set of ordinary differential equations (10). The hydroelastic operator $\mathbf{A}$ depends on V, that in the present analysis is a random function. This last can be expressed by the sum of two contributions: the mean flow component V_0, constant and deterministic, and a random fluctuation $\tilde{V}$, i.e. $V = V_0 + \tilde{V}$. The stochastic nature of $\tilde{V}$ and the solution technique for Eq. (10) is illustrated in the next section.

3.3. Nature of the random perturbation

In the present section the stochastic component $\tilde{V}(t)$ of the inflow velocity is provided as a function of the surface wave perturbation. With reference to realistic seaways, the irregular pattern observed at sea is described in terms of a stationary, zero-mean, Gaussian random process. According to Pierson Moskowitz, the one-sided power-spectral density of the wave elevation at a given location x', is

$$S_\eta(\omega) = \frac{\beta_1 g^2}{\omega^5} \mathrm{e}^{-\beta_1(\beta_2 V_w/w)^4},$$

where x' is the direction of the wave propagation lying on the sea surface, ω is the frequency, V_w is the wind speed over the sea, β_1 and β_2, are suitable constants and g is the gravity acceleration [38]. Following the Airy solution and assuming deep water conditions, the water particle trajectories become very nearly circles with radii that decrease exponentially with depth; the displacement of the water is a random process that can be described by a Rice decomposition (see Section 2) through the superposition of a finite number n of harmonic waves with vertical amplitude A_i at the surface and phase φ_i,

$$\begin{aligned} \xi(x', z, t) &= \sum_{i=1}^{n} A_i \ \sin(kx' - \omega_i t + \varphi_i)\mathrm{e}^{-k_i z}, \\ \eta(x', z, t) &= \sum_{i=1}^{n} A_i \ \cos(k_i x' - \omega_i t + \varphi_i)\mathrm{e}^{-k_i z}, \end{aligned} \tag{13}$$

where ξ and η are the displacement components along x and y axis, respectively (see Fig. 2), ω_i is the frequency sampled in a significant bandwidth, $k_i = 2\pi/\lambda_i$ the wave number and λ_i is the wavelength; the wave amplitudes are given by $A_i = \sqrt{2S_\eta(\omega_i)\Delta\omega}$, where $\Delta\omega$ is the (constant) frequency sampling interval chosen for the assumed spectral discretization. It is worth to point out that, in order to satisfy the model hypothesis, the lowest wavelength $\lambda_{\min}$, corresponding to the

maximum wavenumber $k_{\max}$, must be greater than the depth h, i.e., $\lambda_{\min} > h$. This implies that the maximum considered frequency ω_n in Eq. (13) must be less than $\omega_{\max}$ corresponding (through the dispersion relationship) to $k_{\max}$.

By substituting $x' = -V_0 t$ (changing to the moving hydrofoil reference frame), the dimensionless horizontal $\tilde{V}(t)$ and vertical $\tilde{W}(t)$ velocity perturbations, at $z=h$, are

$$\tilde{V}(t) = \sum_{i=1}^{n} \omega_i A_i \cos[(-k_i V_0 - \omega_i)t + \varphi_i] e^{-k_i h},$$

$$\tilde{W}(t) = -\sum_{i=1}^{n} \omega_i A_i \sin[(-k_i V_0 - \omega_i)t + \varphi_i] e^{-k_i h}.$$

In the following, only head-on perturbations along the x axis are considered, directly affecting the matrix of coefficients $\mathbf{A}(U)$ in Eq. (10). The reader is referred to Ref. [38] for the case of transverse velocity perturbation, where forcing in the presence of external loads dependent on the motion does not change the system coefficients of Eq.(10).

The first Cartesian component of the perturbation velocity shown in the previous equation, $\tilde{V}(t)$, represents an example of a random process when the phases φ_i are randomly generated following a probability density function uniformly distributed in the range $[0, 2\pi]$. Under this condition, Eq. (9) provides a canonical decomposition of the horizontal velocity (see Section 2.1), i.e.,

$$\tilde{V}(t) = \left[\sum_{i=1}^{n} \omega_i A_i \cos(-k_i V_0 + \varphi_i) \cos(\omega_i t) - \omega_i A_i \sin(-k_i V_0 + \varphi_i) \sin(\omega_i t) \right] e^{k_i h},$$

where the random coefficients, $\omega_i A_i \sin(-k_i V_0 + \varphi_i)$, $\omega_i A_i \cos(-k_i V_0 + \varphi_i)$, are statistically independent with zero mean. Moreover it can be shown that the decomposition implies $\tilde{V}(t)$ is stationary [13].

3.4. SPM solution for linear hydroelastic equations

The first Cartesian component of the perturbation velocity $\tilde{V}(t)$ takes also the complex form:

$$\tilde{V}(t) = \mathrm{Re}\left\{ \sum_{i=1}^{n} \gamma_i \Pi_i(t) \right\}, \tag{14}$$

where $\gamma_i = \omega_i A_i e^{-k_i h} e^{-j\varphi_i}$ are random Fourier coefficients, while $\Pi_i(t) = e^{j(k_i V_0 + \omega_i)t}$. Eq. (14) represents a Rice canonical decomposition of the head-on inflow random perturbation, since $E\{\gamma_i\} = 0, E\{\gamma_i \gamma_j^*\} = \delta_{ij}\sigma_{\gamma_i}^2$ (see Eq. (6)). Moreover, Eq. (14) provides $\tilde{V}(t)$ statistically stationary. The presence of $\tilde{V}(t)$, as an argument of $\mathbf{A}$, makes the hydroelastic operator stochastic.

Let us introduce for the sake of simplicity the random coefficients $\Gamma_i = \mathrm{Re}\{\gamma_i\}, \Gamma_{i+n} = \mathrm{Im}\{\gamma_i\}$, having zero mean and correlation matrix $E\{\Gamma_i \Gamma_j\} = \delta_{ij}\sigma_{\Gamma_i}^2$. The SPM outlined in Section 2 applies now to Eq. (10), yielding:

$$\mathbf{A}(t) = \mathbf{A}_0 + \sum_{i=1}^{2n} \Gamma_i \mathbf{A}_{1,i} + \sum_{i,j=1}^{2n} \Gamma_i \Gamma_j \mathbf{A}_{2,ij}, \tag{15}$$

$$\mathbf{y}(t) = \mathbf{y}_0 + \sum_{i=1}^{2n} \Gamma_i \mathbf{y}_{1,i} + \sum_{i,j=1}^{2n} \Gamma_i \Gamma_j \mathbf{y}_{2,ij}, \tag{16}$$

where a Taylor expansion up to the second order in terms of the Γ_i's is used. Note that $\mathbf{y}_{1,i}, \mathbf{y}_{2,ij}$ are unknowns, while $\mathbf{A}_{1,i}, \mathbf{A}_{2,ij}$ are known matrices of derivatives of $\mathbf{A}$ with respect to the Γ_i's. By substituting Eqs. (15) and (16) into Eq. (10), and equating those terms with the same power of Γ_i, the following cascade of deterministic differential equations is obtained:

$$\begin{aligned} &\dot{\mathbf{y}}_0 = \mathbf{A}_0 \mathbf{y}_0, \\ &\dot{\mathbf{y}}_{1,i} = \mathbf{A}_0 \mathbf{y}_{1,i} + \mathbf{A}_{1,i} \mathbf{y}_0, \\ &\dot{\mathbf{y}}_{2,ij} = \mathbf{A}_0 \mathbf{y}_{2,ij} + \mathbf{A}_{1,i} \mathbf{y}_{1,j} + \mathbf{A}_{2,ij} \mathbf{y}_0, \\ &.... \end{aligned} \tag{17}$$

for $i, j = 1, \ldots, 2n$. Once this set of equations is solved, the statistical moments of the solution $\mathbf{y}(t)$ are obtained, as shown in Section 2, as

$$E\{\mathbf{y}\} = \mathbf{y}_0 + \sum_{i=1}^{2n} \sigma_{\Gamma_i}^2 \mathbf{y}_{2,ii}, \quad E\{\mathbf{y}\mathbf{y}^{\mathrm{T}}\} = \mathbf{y}_0 \mathbf{y}_0^{\mathrm{T}} + \sum_{i=1}^{2n} \sigma_{\Gamma_i}^2 (\mathbf{y}_0 \mathbf{y}_{2,ii}^{\mathrm{T}} + \mathbf{y}_{1,} \mathbf{y}_{1,i}^{\mathrm{T}} + \mathbf{y}_{2,ii} \mathbf{y}_0^{\mathrm{T}}). \tag{18}$$

It is important to remark that the obtained results allow the prediction of the statistical behavior of the hydroelastic response of the hydrofoil by solving the linear system of deterministic differential equations (18). The obtained statistical quantities depend, in general, on time. This means that, although the inflow velocity perturbation described by Eq. (14) is a stationary random process, in general the hydroelastic response is not, as shown by Eqs. (18) where both the expected value and the correlation matrix are time dependent.

3.5. A comparison between SPM and MCS solutions

The illustrated approach presents, at least in some cases discussed later in this section, a relevant advantage with respect to a direct Monte Carlo simulation that may require a considerable computational effort. In fact in this case, to obtain significant statistics, Eq. (10) must be solved considering a very large set of different samples of the stochastic process given by Eq. (14). Nevertheless, as shown later on, the results obtained by SPM are in satisfactory agreement with those obtained by the Monte Carlo approach, at least in the limit of small stochastic perturbations affecting the mean flow velocity, otherwise expansions (15) and (16) become inaccurate.

Note that Eq. (17) exhibits, in general, a set of $2n^2 + 3n + 1$ vector equations (considering the symmetry of the third set of equations (17)), where n is the number of frequency samples used in Eq. (13). However, Eq. (18) shows that, when the random perturbation affecting the hydroelastic operator can be reduced to a canonical form, i.e., $E\{\Gamma_i \Gamma_j\} = \delta_{ij} \sigma_{\Gamma_i}^2$, as in the present case, the estimate of both the mean and the correlation matrix of the solution $\mathbf{y}$ does not need the contribution of $\mathbf{y}_{2,ij}$for any pair of index i, j: it is sufficient to solve the third set of Eq. (17) only for $\mathbf{y}_{2,ii}$. This represents a great simplification of the problem, since the statistics given by Eqs. (18), can be obtained by solving $4n + 1$ vector differential equations only.

On the other hand when using a MCS, the number N of simulations performed in Eq. (10) depends on the accuracy required in the estimate (at each time) of the mean and the variance of the studied process.

In the following a comparison between the exact solution and those obtained by MCS and SPM will be performed on a special form of the prototype Eq. (7):

$$\dot{y}(t) + ay(t) = a, \quad y(0) = 0, \tag{19}$$

where the parameter a is a random coefficient and $p(a)$ is the associated pdf. The exact statistical solution is determined to provide a benchmark for an effective comparison between SPM and MCS. The solution of the considered equation is $y(t) = 1 - e^{-at}$, therefore, the mth order statistical moment of y is provided by

$$E\{y^m\} = \int_{-\infty}^{+\infty} (1 - e^{-at})^m p(a)\, da \tag{20}$$

that, at least for some pdf, returns a closed-form expression of the moment. The pdf distribution here considered is

$$p(a) = \frac{\gamma}{2\sigma_a}\left[1 - \cos\frac{\pi(a - a_0 + \sigma_a/\gamma)}{\sigma_a/\gamma}\right]$$

along the interval $|a - a_0| \leqslant \sigma_a/\gamma$, where $a_0 = E\{a\}$, $\sigma_a = E\{(a - a_0)^2\}$ and $\gamma = \sqrt{(\pi^2 - 6)/(3\pi^2)}$. In this case one obtains, by using Eq. (20),

$$E\{e^{-mat}\} = \pi^2 e^{-m((\sigma_a/\gamma)+a_0)t}\left(e^{2m(\sigma_a/\gamma)t} - 1\right) \Big/ 2m\left[\pi^2 \frac{\sigma_a}{\gamma} t + m^2\left(\frac{\sigma_a}{\gamma} t\right)^3\right].$$

With these expressions, the statistics of the exact solution up to the second order is provided in the form:

$$E\{y\} = \bar{y} = 1 - E\{e^{-at}\}, \tag{21}$$

$$E\{(y - \bar{y})^2\} = \sigma_y^2 = 2\bar{y} - \bar{y}^2 - 1 + E\{e^{-2at}\}. \tag{22}$$

Next, the statistic solution by SPM of the same Eq. (19) will be obtained. Assume that the random coefficient a has the form (see Eq. (2)):

$$a = a_0(1 + \varepsilon), \tag{23}$$

where a_0 is deterministic (the mean value of a) and ε is a small random parameter with zero mean and $\sigma_\varepsilon = \sigma_a/a_0$. The approximated solution—in perturbation sense—of Eq. (19) can be expressed as

$$y(t) = \sum_{k=0}^{n} \varepsilon^k y_k(t). \tag{24}$$

By introducing Eqs. (23) and (24) into Eq. (19) and ordering with respect to the power of ε, one has

$$y_0 + a_0 y = a_0,$$

$$\dot{y}_1 + a_0 y_1 = a_0(1 - y_0),$$
$$\dot{y}_j + a_0 y_j = -a_0 y_{j-1}, \quad j = 2, n.$$

The solutions of the previous set of equations are given in closed form as

$$y_0(t) = 1 - \mathrm{e}^{-a_0 t}, \quad y_j(t) = \mathrm{e}^{-a_0 t}(-1)^{j-1}(a_0 t)^j / j! \quad j = 1, 2, \ldots, n. \tag{25}$$

By using Eqs. (24) and (25) one has

$$y(t) = 1 - \mathrm{e}^{-a_0 t}\left[1 - \sum_{k=1}^{n}(-1)^{k-1}\frac{(a_0 t)^k}{k!}\varepsilon^k\right],$$

i.e.

$$E\{y^m\} = E\left\{\left[1 - \mathrm{e}^{-a_0 t}\left(1 - \sum_{k=1}^{n}(-1)^{k-1}\frac{(a_0 t)^k}{k!}\varepsilon^k\right)\right]^m\right\}.$$

For $n = 2$ and neglecting terms of order higher than ε^2, one obtains

$$E\{y_{\mathrm{SPM}}\} = \bar{y}_{\mathrm{SPM}} = y_0 + \sigma_\varepsilon^2 y_2,$$
$$E\left\{\left(y_{\mathrm{SPM}} - \bar{y}_{\mathrm{SPM}}\right)^2\right\} = \sigma_{y\mathrm{SPM}}^2 = \sigma_\varepsilon^2 y_1^2. \tag{26}$$

On the basis of Eqs. (21), (22), (25), and (26), Figs. 3 and 4 show the comparison between the exact solution and the SPM solution in terms of mean value and standard deviation, respectively for $a_0 = 1$, and $\sigma_\varepsilon = 0.15$: note that a good agreement is found. In Fig. 5 the error both for the mean value and the standard deviation is shown.

These results are preliminary for the comparison between SPM and MCS. When performing a MCS, at any time t the statistics of $y(t) = 1 - \mathrm{e}^{-at}$ can be studied. Consider initially the mean value of the solution. An estimate of the mean is given by the arithmetic average $\tilde{y}(t)$ of the samples of $y(t) = 1 - \mathrm{e}^{-at}$ at each time t:

$$\tilde{y}(t) = \sum_{i=1}^{N}\frac{1 - \mathrm{e}^{-a_i t}}{N},$$

where the a_i's are stochastic samples of a and $\tilde{y}(t)$ is a random variable that provides an estimate of $E\{y\}$. The analysis of the errors implied in this estimate is the key to compare the MCS results with those given by SPM. Since $\tilde{y}(t)$ is the sum of N terms having identical distribution, for N large enough (20–30 samples) the central limit theorem can be applied and $\tilde{y}(t)$ can be approximately considered as a random variable having normal distribution [3,13]. Let β the probability that $\left|\tilde{y} - E\{y\}\right| < I_\varepsilon$, i.e., that the exact mean is included in the interval of centre $\tilde{y}(t)$ and range I_ε.

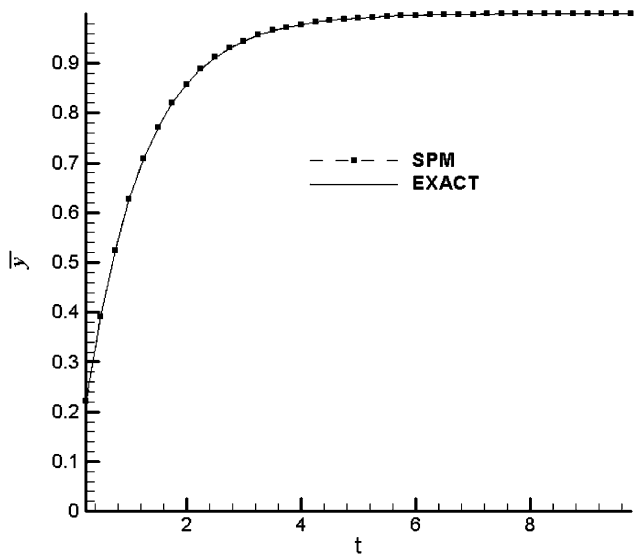

Fig. 3. Comparison between the exact solution and the SPM solution in terms of mean value ($a_0 = 1$, and $\sigma_\varepsilon = 0.15$).

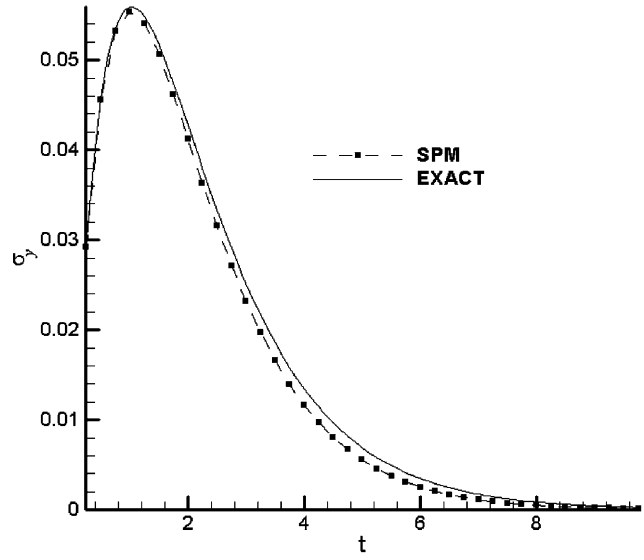

Fig. 4. Comparison between the exact solution and the SPM solution in terms of standard deviation ($a_0 = 1$, and $\sigma_\varepsilon = 0.15$).

Since $\tilde{y}(t)$ has a normal distribution, one has

$$\beta = 2\int_0^{\varepsilon} \frac{1}{\sqrt{2\pi\sigma_{\tilde{y}}^2}} \mathrm{e}^{-\frac{1}{2}(\tilde{y}/\sigma_{\tilde{y}})^2} \mathrm{d}\tilde{y} = \mathrm{Erf}\left(\frac{I_\varepsilon}{\sqrt{2}\sigma_{\tilde{y}}}\right)$$

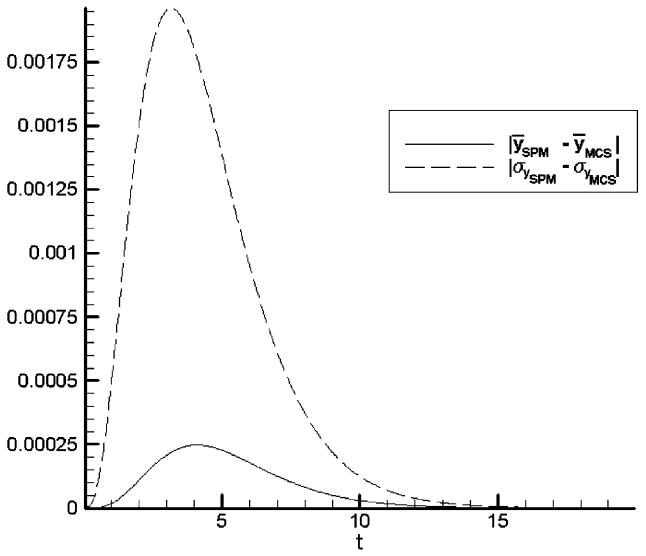

Fig. 5. Comparison between the exact solution and the SPM solution in terms of the error both for the mean value and the standard deviation.

being $\sigma_{\tilde{y}}$ the estimate of the variance of y:

$$\sigma_{\tilde{y}}(t) = \sqrt{\frac{\sum_{k=1}^{N}(1 - e^{-a_i t} - \tilde{y})^2}{N-1}}$$

Thus, the bandwidth I_ε of the interval is

$$I_\varepsilon = \sqrt{2}\mathrm{Erf}^{-1}(\beta), \quad \sigma_{\tilde{y}}(t) = A_\beta \sigma_{\tilde{y}}(t).$$

Once a probability β is assumed, A_β is determined through the inverse of the Erf function: e.g., $\beta = 0.90$, implies $A_\beta \cong 1.5$ (see [13]). Since $\sigma_{\tilde{y}}(t) - \sigma_y(t)/\sqrt{N}$ the confidence interval amplitude $I_\beta = 2I_\varepsilon$ is given by

$$I_\beta \cong \frac{3\sigma_y}{\sqrt{N}}.$$

This expression provides the error range (with a probability β) associated to the estimate $\tilde{y}(t)$ of the mean value $E\{y\}$ at a given time t.

The same line can be used to provide the confidence interval of the standard deviation $\sigma_{\tilde{y}}$. In this case it can be shown that the confidence interval has amplitude, [13]:

$$I_\beta = \sqrt{\frac{\mu_4(t)}{N} - \frac{(N-3)\sigma_y^2(t)}{N(N-1)}},$$

where $\mu_4(t)$ is the fourth-order moment of y.

On the basis of the previous results, a comparison between the statistical moments of the solution provided by the SPM and the MCS will be performed. The error introduced in the

estimate of the mean by the SPM approximation can be defined by

$$\epsilon^{(1)}_{\mathrm{SPM}}(t) = \left|\bar{y}(t) - \bar{y}_{\mathrm{SPM}}(t)\right|,$$

whilst that introduced by the MCS yields

$$\epsilon^{(1)}_{\mathrm{MCS}}(t) = \frac{3\sigma_y(t)}{\sqrt{N}}.$$

Moreover, an analogous error associated with the standard deviation estimate can be introduced as in the following:

$$\epsilon^{(2)}_{\mathrm{SPM}}(t) = \left|\sigma_y(t) - \sigma_{y_{\mathrm{SPM}}}(t)\right|,$$

whereas for the MCS, one has

$$\epsilon^{(2)}_{\mathrm{MCS}}(t) = 2A_\beta\sqrt{\frac{\mu_4(t)}{N} - \frac{(N-3)\sigma_y^2(t)}{N(N-1)}} \approx 2A_\beta\sqrt{\frac{\mu_4(t) - \sigma_y^2(t)}{N}},$$

the last expression being valid if N is large enough. The previous estimates of the errors allow a direct comparison between the SPM and MCS accuracy in terms of the number N of runs to be employed by the MCS. One can provide the order of magnitude of the number of runs needed by the MCS to obtain an accuracy of the statistical estimate comparable with that provided by the SPM simulation by equating the expressions previously found for the errors:

$$\epsilon^{(1)}_{\mathrm{SPM}}(t) = \epsilon^{(1)}_{\mathrm{MCS}}(t) \;\Rightarrow\; N = \left[\frac{2A_\beta\sigma_y(t)}{|\bar{y}(t) - \bar{y}_{\mathrm{SPM}}(t)|}\right]^2, \tag{27}$$

$$\epsilon^{(2)}_{\mathrm{SPM}}(t) = \epsilon^{(2)}_{\mathrm{MCS}}(t) \;\Rightarrow\; N = \left[\frac{2A_\beta\sqrt{\mu_4(t) - \sigma_y^2(t)}}{|\sigma_y(t) - \sigma_{y_{\mathrm{SPM}}}(t)|}\right]^2.$$

Eq. (27) provides a simple way for a quantitative comparison between the computational time required by the SPM and MCS in order to obtain the same statistical accuracy for the respective solutions. If N provided by Eq. (27) is evaluated at a given time t_0 and for a given a_0, it appears, considering Eqs. (21) and (22), that the required N is a function of σ_0 only. The SPM solution needs a computational time T_{SPM} proportional to n (number of harmonics in the Rice expansion, for the canonical case), while MCS needs a computational time T_{MCS} proportional to N: thus, the ratio $T_{\mathrm{MCS}}/T_{\mathrm{SPM}}$ is proportional to N/n. Fig. 6 shows the function $N(\sigma_a)$ for $t_0 = 1, a_0 = 1$, that given n, provides a quantity proportional to $T_{\mathrm{MCS}}/T_{\mathrm{SPM}}$ as a function of σ_0. This curve illustrates clearly the computational advantage presented by SPM with respect to MCS.

Summarizing the previous results, it is concluded that conditions favoring use of the SPM in preference to MCS, are:

- the random perturbation affecting the system's response can be represented by a canonical decomposition: if it is not, the computational cost scales as n^2 instead of n; this implies that a stationary stochastic inflow perturbation allows a great simplification;

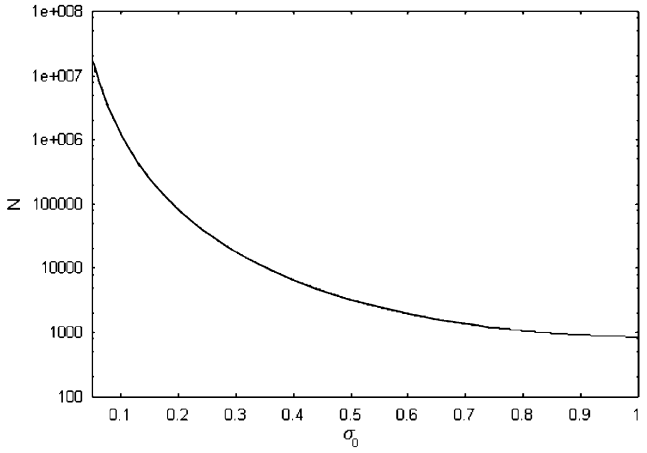

Fig. 6. Function $N(\sigma_a)$ for $t_0 = 1, a_0 = 1$.

- the random perturbation is small with respect to the deterministic part of the process: this permits a great advantage of SPM with respect to MCS in terms of computational time as shown by Fig. 6;
- the number of harmonics n of the discrete power spectrum of the random disturbance is not too high; clearly spectra having energy concentrated in a dominant peak, as in the case of the Pierson–Moskowitz spectrum, allows a reduction of n, with respect to the case of rather flat spectra.

Under these conditions, the SPM solution permits in general a considerable saving of computational time with respect to a direct MCS, having a comparable accuracy in the estimate of the mean and the standard deviation.

4. Numerical results

In this section, some results related to the free response problem obtained by the stochastic perturbation method are presented and compared with those determined via Monte Carlo simulations.

The first application refers to a two degrees of freedom typical section in Section 3.1. Eqs. (9) of the typical section are here characterized by the following dimensionless hydrofoil parameters:

$$x_\alpha = 0.3, \quad \mu = 0.172, \quad r_\alpha = 0.651, \quad a_h = -0.3, \quad \Omega = 0.26.$$

It is worthwhile to note that the mass ratio coefficient $\mu = 0.172$ has a very small value with respect to those commonly found in aeroelasticity but is typical of cases of hydroelastic interest. More precisely, the considered set of parameters represents a reasonable approximation of a hydroelastic model for the submerged control surface of a high-speed marine vehicle. The other parameters are rather close to the typical values usually met for wing structures.

The transient system response to the initial condition $\mathbf{y}^{\mathrm{T}}(0) = (0, 0, 0, 0, 0.01, 0)$ is investigated corresponding to a given initial angular pulse.

The previous theoretical analysis shows how the statistics of the state space vector can be determined. The heave and pitch motion statistics, in terms of mean value and standard deviation, are predicted by SPM. Since the method implies a perturbation technique (see discussion in Section 3.3), reliable results are expected only when reasonably small stochastic perturbations of the flow speed are considered. The order of magnitude of the stochastic fluctuations with respect to the mean flow velocity is kept by the dimensionless parameter $\sigma_{\tilde{U}}/U_0$, where $U_0 = 0.1\ U_D$ and $U_D = 0.426$ is the limit, non-dimensional divergence speed. Thus, when increasing $\sigma_{\tilde{U}}/U_0$, more severe test conditions for SPM are approached so that the sensitivity of the method with respect to $\sigma_{\tilde{U}}/U_0$ is investigated.

The Pierson–Moskowitz spectrum is specified for a wind velocity of 15 m/s, with a peak frequency about 1 rad/s, and a corresponding dominant wavelength $\lambda \approx 60$ m; the hydrofoil chord is 0.43 m, and the assumed depth of the wing $h = 2.24$ m. These choices respect the condition $\lambda > h > \kappa 2b$, discussed in Section 3, and utilize realistic values obtained by the finite-element model shown later in this section. The number of frequency samples is $n = 100$ lying in the frequency range $0 < \omega < 7$ rad/s.

Finally, note that the time-step to be used in the numerical integration of Eq. (17) by the fourth-order Runge–Kutta method—or solving Eq. (10) by MCS with the same time-stepping algorithm—is generally a fraction of the smallest period $T_n = 2\pi/n\Delta\omega$ associated with the highest considered frequency $n\Delta\omega$ in the Pierson–Moskowitz spectrum. Since the phenomenon must be simulated during a time interval including the largest period in the spectrum $T_1 = 2\pi/\Delta\omega$, it follows that each simulation needs a number of integration time steps simply proportional to $T_1/T_n = n$.

The first set of simulation is performed for $\sigma_{\tilde{U}}/U_0 = 0.149$. In Figs. 7 and 8, the time histories of the mean values of the pitch and heave are given, respectively. In each plot two curves are represented. The first is obtained by MCS whilst the second one is obtained by SPM. The SPM curve completely merges that obtained by the MCS in all over the considered time window. The MCS are performed on a set of samples large enough to obtain a statistic convergence of the results.

In Figs. 9 and 10 corresponding results are referred to the standard deviation. Again a good agreement between MCS and SPM results is observed, although a different level of accuracy with respect to the mean value prediction is apparent.

A second set of simulations is performed for $\sigma_{\tilde{U}}/U_0 = 0.265$. In Figs. 11 and 12, again the time histories of both the mean value of the pitch and plunge are given, respectively. The mean values (Fig. 11) are in good agreement, although a more evident difference between MCS and SPM with respect to the case shown in Fig. 3 appears, as expected. In Figs. 13 and 14, the standard deviations of both plunge (Fig. 13) and pitch (Fig. 14) response are represented showing a larger difference with respect to the case of Figs. 9 and 10.

In the following, the SPM procedure is applied to the actual modeling of a new concept vessel SEABUS-HYDAER. This is a Surface-Piercing, Hydrofoil-Controlled, Wing-In-Ground Effect (SP-HC-WIG) vehicle designed to transport payload at cruising speeds beyond the limit of conventional high-speed ships. In order to keep the desired sea-wing clearance and improve the craft stability, the SEABUS-HYDAER is equipped with three submerged control surfaces

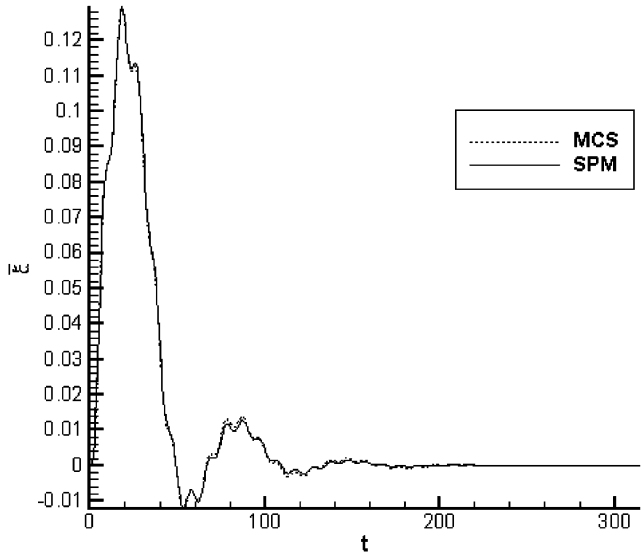

Fig. 7. Time-history of the mean value of plunge: comparison between SPM and MCS ($\sigma_{\tilde{U}}/U_0 = 0.149$).

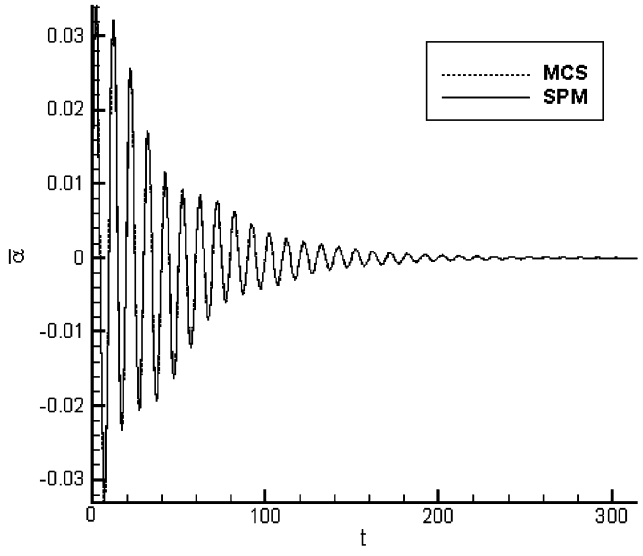

Fig. 8. Time-history of the mean value of pitch: comparison between SPM and MCS ($\sigma_{\tilde{U}}/U_0 = 0.149$).

(hydrofoils), connected to the wing-fuselage by vertical, water-piercing struts. Thus, a faster time response to control inputs is obtained by the use of hydrofoils instead of airfoils due to the higher density of water.

The three-dimensional wing of the SEABUS analyzed here has a geometry characterized by a wing root equal to 0.60 m, a chord tip equal to 0.26 m, and an half-span length equal to 1.65 m.

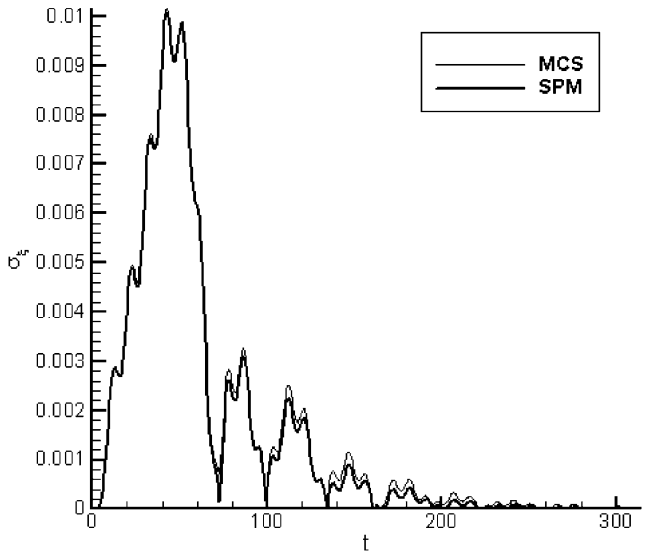

Fig. 9. Time-history of standard deviation of plunge: comparison between SPM and MCS ($\sigma_{\tilde{U}}/U_0 = 0.149$).

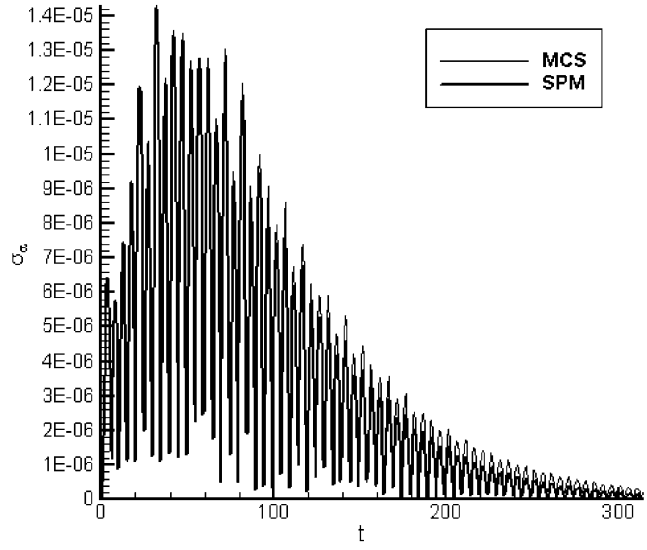

Fig. 10. Time-history of standard deviation of pitch: comparison between SPM and MCS ($\sigma_{\tilde{U}}/U_0 = 0.149$).

The wing operates at a depth 2.24 m, a condition that respects the hypotheses $\lambda > h > \kappa 2b$, when the sea spectrum is the same considered in the previous results.

The structural analysis of the SEABUS wing has been performed by using the finite element MSC NASTRAN commercial code: two spars located at 20% and 80% of the chord length, respectively, have been considered; the structure is composed of isotropic material, an aluminum alloy (7975 type) with Young's modulus equal to 72 GPa, a Poisson ratio of 0.3 and a material

Table 1
Control surface characteristic thickness

Front spar	10 mm
Rear spar	8.0 mm
Front skin	7.0 mm
Middle skin	5.0 mm
Rear skin	3.0 mm

Table 2
Numerical natural frequency of the SEABUS control surface

Mode number	Frequency (Hz)
1	26.47
2	109.17
3	168.27
4	190.94
5	217.67

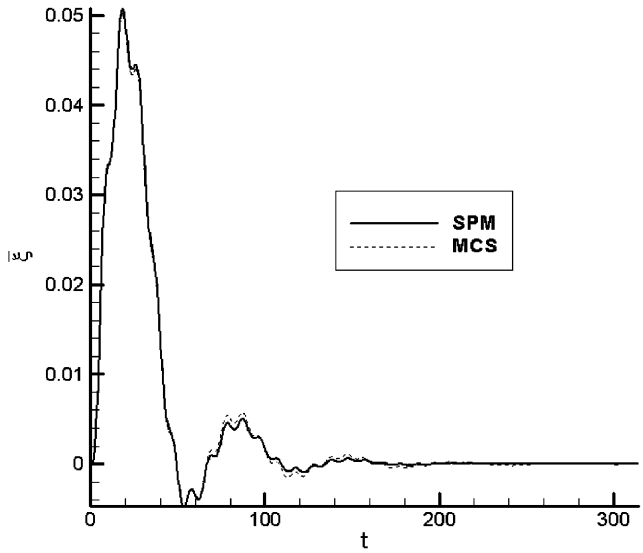

Fig. 11. Time-history of the mean value of plunge: comparison between SPM and MCS ($\sigma_{\tilde{U}}/U_0 = 0.265$).

density of 2800 kg/m^3. The thickness of several portions of the skin and the spars are presented in Table 1.

The finite element analysis is performed by using 20 shell elements in the half-span direction, 25 shell elements in chord-wise direction, and 4 shell elements are used for the spares in the direction

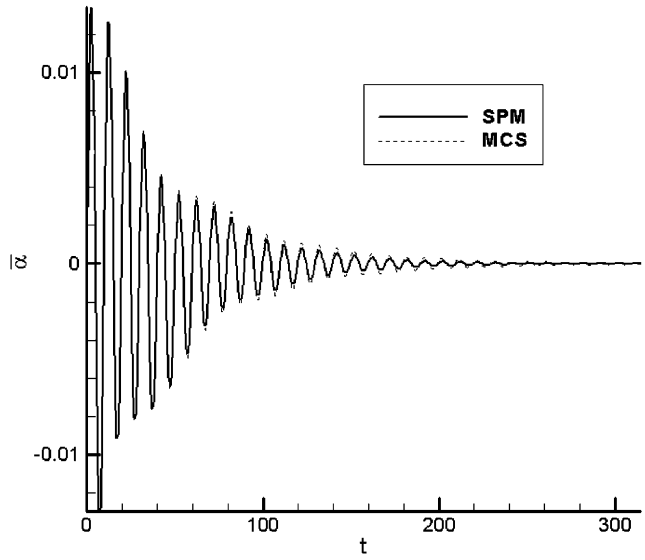

Fig. 12. Time-history of the mean value of pitch: comparison between SPM and MCS ($\sigma_{\tilde{U}}/U_0 = 0.265$).

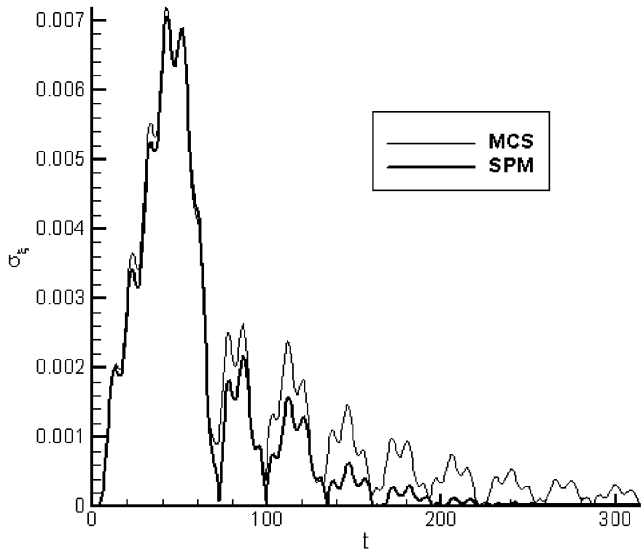

Fig. 13. Time-history of standard deviation of plunge: comparison between SPM and MCS ($\sigma_{\tilde{U}}/U_0 = 0.265$).

perpendicular to the wing plane (1160 elements and 1176 nodes). The wing has been cantilevered and the first five natural frequencies are depicted in Table 2.

Figs. 14–19 show the corresponding dry mode shapes. They reveal a typical mixed bending-torsion nature. The flutter instability, when a water density $\rho = 1000$ kg/m^3 is assumed, occurs for $U_F = 70.4$ m/s with a critical flutter frequency $f_F = 24.84$ Hz (i.e., apparently the critical flutter mode consists mainly of the first mode of free vibration).

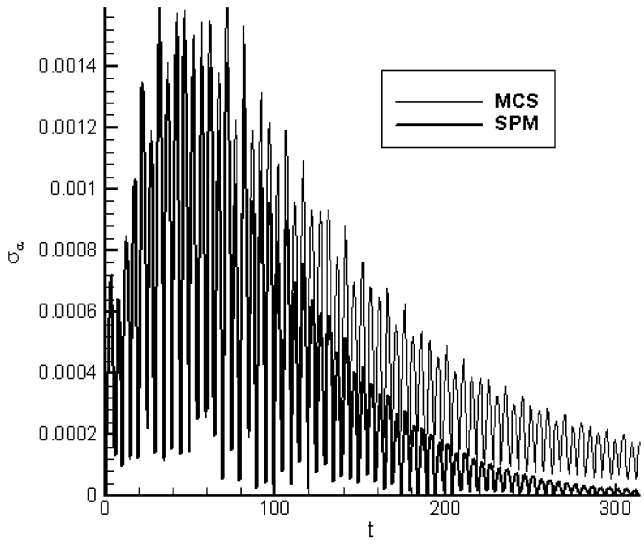

Fig. 14. Time-history of standard deviation of pitch: comparison between SPM and MCS ($\sigma_{\tilde{U}}/U_0 = 0.265$).

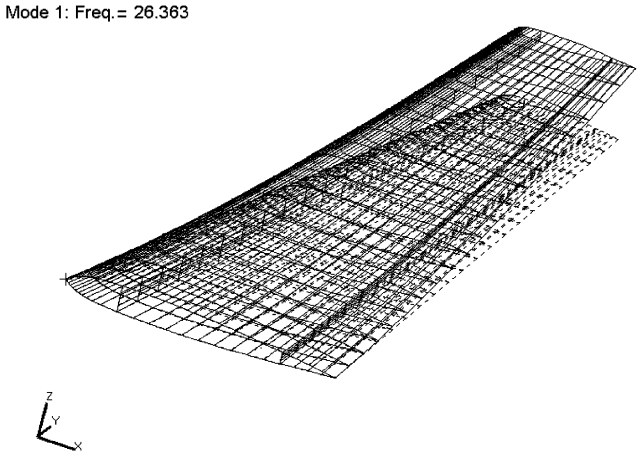

Fig. 15. First mode shape of the Seabus control surface.

Next, SPM vs MCS simulations are provided for the five-mode hydroelastic model of the SEABUS wing. For this case, a Runge–Kutta method was employed too to integrate the related equations. On the basis of the approach given in Section 3, the vertical displacement at the trailing edge tip of the wing is considered. Initial conditions are $\mathbf{q}(0) = 0$ and $\dot{\mathbf{q}}(0) = 15\{2.510^{-1}, -2.710^{-3}, 2.310^{-3}, 0.0, 1.310^{-3}\}^{\mathrm{T}}$ and the Pierson-Moskowitz spectrum corresponds to a wind velocity $V_W = 10$ m/s. Figs. 20 and 21 depict, respectively, the mean value and the standard deviation of the vertical displacement of the trailing edge tip point obtained by the SPM approach. The comparison with the results obtained with the MCS is presented in Fig. 22 which shows a 3σ analysis based on the prevision of the previous SPM analysis: indeed, the bounding

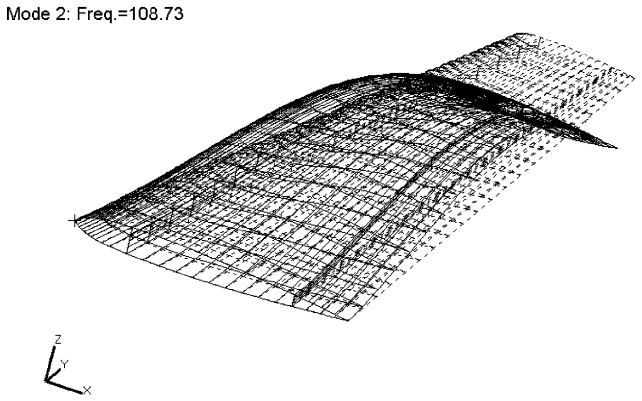

Fig. 16. Second mode shape of the Seabus control surface.

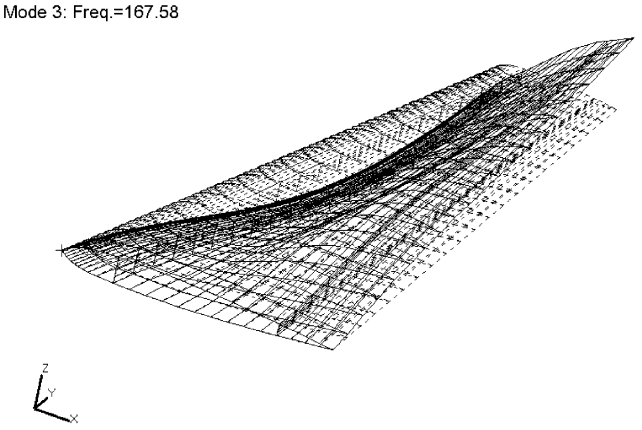

Fig. 17. Third mode shape of the Seabus control surface.

curves are obtained adding to the mean value curve (see Fig. 20) the $\pm 3\sigma(t)$ curves (see Fig. 21). Note that the curves obtained with the MCS all lie in this range, as theoretically expected.

5. Conclusions

This paper proposes the use of a stochastic perturbation approach, in conjunction with a Rice expansion of the random inflow perturbation, to study fluid–structure interaction problems. Two different models have been studied: the first refers to a typical hydrofoil section, the second to an actual control surface modeled by using a FEM for the structure coupled with an unsteady lifting surface panel method for the hydrodynamics. In the analysis of both models it has been shown how the presence of random head-on inflow perturbations makes the hydroelastic operator stochastic. The analysis cannot be achieved in the frame of the classical theory of random

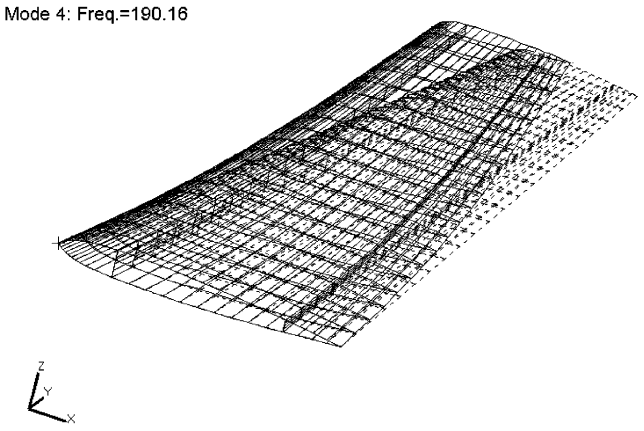

Fig. 18. Fourth mode shape of the Seabus control surface.

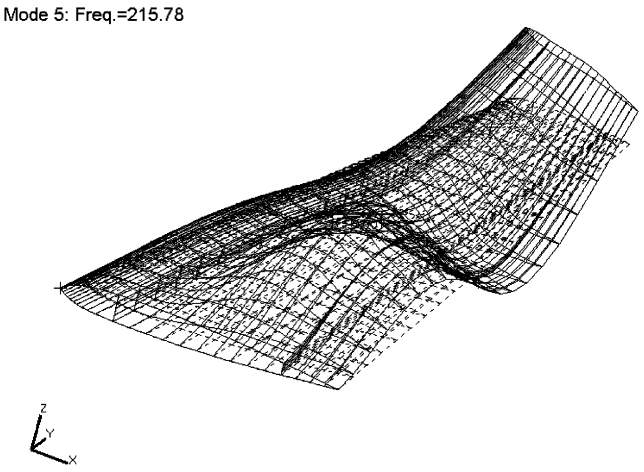

Fig. 19. Fifth mode shape of the Seabus control surface.

vibrations because of the kind of randomness involved: it affects the coefficients of the fluid–structure operator, leading the problem into the field of differential equations with stochastic coefficients. Although a direct solution of the problem by a Monte Carlo approach is always possible, it can lead to high computational costs in order to achieve statistically significant results. An interesting alternative lies in the use of the SPM proposed here. At least under some conditions, which seem to be met in a wide class of fluid-structural problems of practical interest, the computational advantage of this method is apparent, and the results are directly obtained in terms of the desired statistical quantities. Moreover, the SPM can be used without placing particular restriction on the nature of the problem. In fact, as it has been shown, it applies for the analysis of statistically nonstationary response. Moreover, although this is not the case considered here, fluid–structure interaction problems characterized by a nonlinear formulation could be

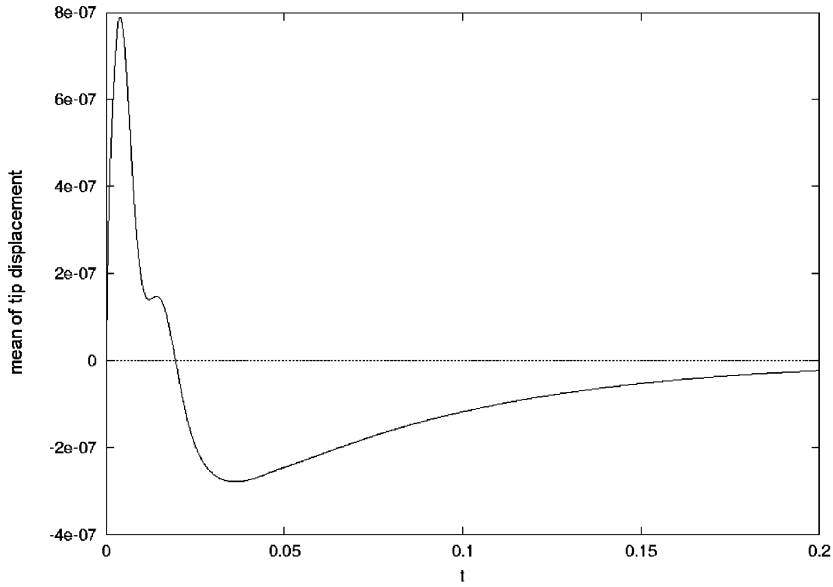

Fig. 20. Time-history of the mean value for the vertical displacement at the trailing edge tip point.

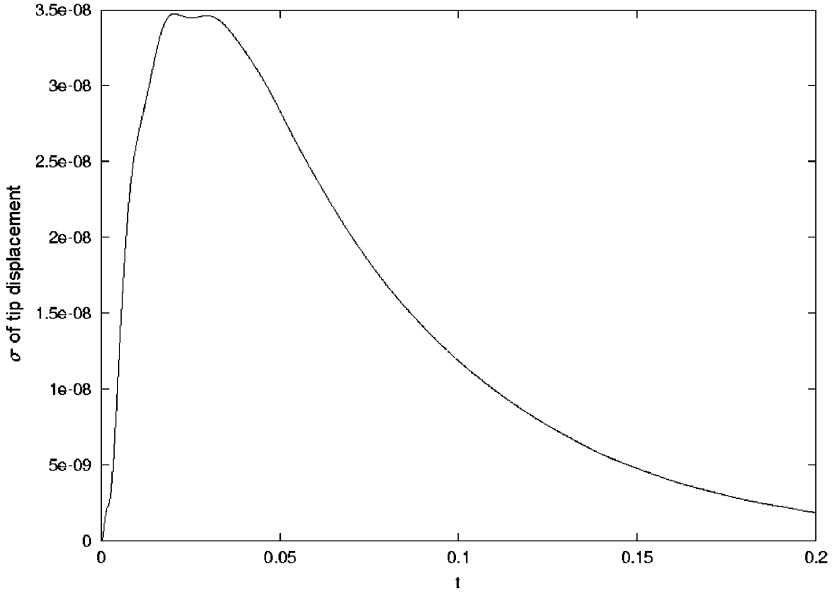

Fig. 21. Time-history of the standard deviation for the vertical displacement at the trailing edge tip point.

analyzed as well. Nevertheless, one of the main requirements needed to a successful approach of SPM is the possibility of a canonical decomposition of the input random process. However, in the context of engineering problems, this requirement does not appear to place serious restrictions on the use of the proposed technique.

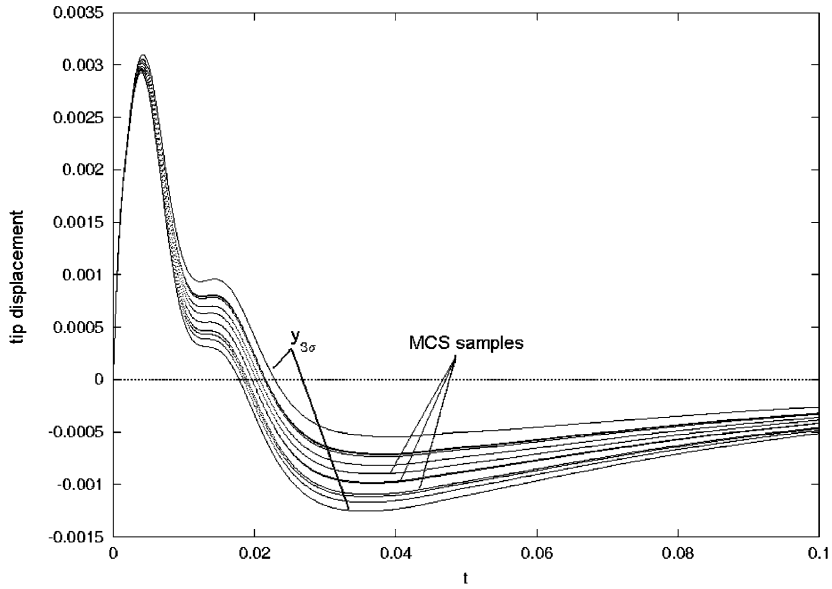

Fig. 22. 3σ analysis of the vertical displacement at the trailing edge tip point and comparison with MCS.

Therefore it seems that SPM deserves to be developed and applied to a wider class of fluid–structure interaction problems. It offers a promising alternative when Monte Carlo methods encounter computational difficulties.

Acknowledgments

This paper is dedicated to the memory of our colleague and friend Dr. Maurizio Landrini, who died unexpectedly the morning of 26th June 2003 in Rome.

Appendix A

In this appendix it is shown how the stochastic response of a system can have a decaying amplitude even in the presence of a steady-state wave forcing, appearing in the equation as a random time-dependent stiffness coefficient. Consider the homogeneous equation $J\ddot{\theta} + C\dot{\theta} + K'\theta = 0$, where $K'(t) = K - q(U, u_x(t))$ is a random process, it belongs to the class of Ito's type equations. The properties of its solution can be determined by the equation of moments [4 , pp. 228–231]. If $K' = K - q(U, u_x)$, sum of the constant deterministic stiffness and a random time-dependent Gaussian stiffness, then the statistical moments

$$m_{jk}(t) = E\left\{X_1^j(t)X_1^k(t)\right\}, \quad \theta = X_1, \quad \dot{\theta} = X_2$$

of the solution obey the equations

$$\begin{Bmatrix} \dot{m}_{10} \\ \dot{m}_{01} \end{Bmatrix} = \begin{bmatrix} 0 & 1 \\ -K/J & -C/J \end{bmatrix} \begin{Bmatrix} m_{10} \\ m_{01} \end{Bmatrix} \quad \text{for the first-order moments,}$$

$$\begin{Bmatrix} \dot{m}_{20} \\ \dot{m}_{11} \\ \dot{m}_{02} \end{Bmatrix} = \begin{bmatrix} 0 & 2 & 0 \\ -K/J & -C/J & 1 \\ 2D_{11}/J & -2K/J & -2C/J \end{bmatrix} \begin{Bmatrix} m_{20} \\ m_{11} \\ m_{02} \end{Bmatrix} \quad \text{for the second-order moments,}$$

where D_{11} is the standard deviation of q. The first-order moments are characterized by a decaying time trend: they tend to zero when t tends to infinity. In fact, the eigenvalues of the first-order moment matrix exhibit always negative real parts. The analysis of the second-order moments shows the same property as it can be easily numerically verified. This implies that the equation of motion of this simplified wing section with random Gaussian stiffness, has a long-term response whose moments (up to the second order) go to zero as time increases, implying clearly that the response of the wing section is damped even in presence of a steady-state wave forcing, appearing in the equation as a random time-dependent stiffness coefficient.

References

[1] M. Shinozuka, G. Deodatis, Response variability of stochastic finite element systems, Technical Report, Department of Civil Engineering, Columbia University, New York, 1986.

[2] R.G. Ghanem, P. Spanos, *Stochastic Finite Elements: a Spectral Approach*, Springer, Berlin, 1991.

[3] V.V. Bolotin, *Random Vibrations of Elastic Systems*, Martinus Nijhoff, The Hague, The Netherlands, 1984.

[4] T.T. Soong, *Random Differential Equations in Science and Engineering*, Academic Press, New York, 1973.

[5] T.T. Soong, M. Grigoriu, *Random Vibration of Mechanical and Structural Systems*, Prentice-Hall, Englewood Cliffs, NJ, 1989.

[6] Y.K. Lin, G.Q. Cai, Stochastic analysis of nonlinear systems, in: S.G. Braun, D.J. Ewins, S.S. Rao (Eds.), *Encyclopedia of Vibration*, Academic Press, New York, 2002.

[7] Z. Schuss, *Theory and Applications of Stochastic Differential Equations*, Wiley, New York, 1975.

[8] S.O. Rice, Mathematical analysis of random noise, *Bell System Techniques Journal*, 23 (1954) 282–332, 24 (1954) 46–156. Reprinted in selected papers on *Noise and Stochastic Processes*, Dover, New York, 1954.

[9] L. Meirovitch, *Elements of Vibration Analysis*, McGraw-Hill, Singapore, 1986.

[10] E.H. Dowell, *A Modern Course in Aeroelasticity*, Kluwer Academic Publishers, Dordrecht, 1992.

[11] F.M. Hoblit, *Gust Loads on Aircraft: Concepts and Applications*, AIAA Educational Series, Washington, DC, 1988.

[12] W.P. Rodden, E.H. Johnson, *MSC/NASTRAN—Aeroelastic Analysis, User's Guide Ver. 68*, The Macneal-Schwendler Corporation, 1994.

[13] L. Ventsel, *Teoria delle Probabilità*, MIR, Moscow, 1983 (in Italian).

[14] J.L. Bogadanov, F. Kozin, Moments of the output of linear random systems, *Journal of the Acoustical Society of America* 34 (1962) 1063–1068.

[15] G. Cumming, Derivation of the moments of a continuous stochastic system, *International Journal of Control* 5 (1967) 85–90.

[16] G. Adomian, Random operator equations in mathematical physics, *Journal of Mathematical Physics* 11 (1970) 1069–1084.

[17] R.C. Bourret, Propagation of randomly perturbed fields, *Canadian Journal of Physics* 40 (1970).

[18] D. Xiu, G.E. Karniadakis, The Wiener–Askey polynomial chaos for stochastic differential equations, *Journal of Scientific Computing* 24 (2) (2002) 619–644.
[19] X. Robert, Y. Spanos, *Random Vibration and Statistical Linearization*, Wiley, New York, 1990.
[20] N. Wiener, The homogeneous chaos, *American Journal of Mathematics* 60 (1938) 897–936.
[21] M. Jardak, C.H. Su, G.E. Karniadakis, Spectral polynomial chaos solutions of the stochastic advection equation, *Journal of Scientific Computing* 17 (1–4) (2002) 319–338.
[22] D. Xiu, D. Lucor, C.H. Su, G.E. Karniadakis, Stochastic modelling of flow-structure interactions using generalized polynomial chaos, *Journal of Fluid Engineering* 124 (2002) 51–59.
[23] T.T. Soong, J.L. Bogdanoff, On the natural frequencies of a disordered linear chain of N degrees of freedom, *International Journal of Mechanical Science* 5 (1963) 237–265.
[24] T.T. Soong, J.L. Bogdanoff, On the impulsive admittance and frequency response of a disordered linear chain of N degrees of freedom, *International Journal of Mechanical Science* 6 (1964) 225–237.
[25] A.H. Nayfeh, *Perturbation Methods*, Wiley, New York, 1973.
[26] M. Karpel, Design for active flutter suppression and gust alleviation using state-space aeroelastic modelling, *Journal of Aircraft* 19 (3) (1982) 221–227.
[27] L. Morino, F. Mastroddi, R. De Troia, G.L. Ghiringhelli, P. Mantegazza, Matrix fraction approach for finite-state aerodynamic modeling, *AIAA Journal* 33 (4) (1995) 703–711.
[28] G. Krall, *Meccanica delle Vibrazioni*, Veschi, Rome, 1970 (in Italian).
[29] W.J. Pierson, L. Moskowitz, A proposed spectral form for fully developed wind seas based on the similarity theory of S.A. Kitaigorodskii, *Journal of Geophysics Research* 69 (1964) 5181–5190.
[30] L.K. Wadlin, C.L. Shuford, J. McGehee, A theoretical and experimental investigation of the lift and drag characteristics of hydrofoils at subcritical and supercritical speeds, *Naca Technical Report* 1232 (1961) 661–671.
[31] T. Theodorsen, General theory of aerodynamic instability and the mechanism of flutter, *Naca Report* 496 (1935) 413–433.
[32] R.T. Jones, The unsteady lift of a wing of finite aspect ratio, *Naca Report* 681 (1940) 31–36.
[33] Y.C. Fung, *An Introduction to the Theory of Aeroelasticity*, Dover, New York, 1969.
[34] R.L. Blisplinghoff, H. Ashley, *Principles of Aeroleasticity*, Wiley, New York, 1962.
[35] D. Dessi, F. Mastroddi, L. Morino, Limit-cycle stability reversal near a Hopf bifurcation with aeroelastic applications, *Journal of Sound and Vibrations* 256 (2) (2002) 347–365.
[36] D.C. Poirel, S.J. Price, Post-instability behaviour of structurally nonlinear airfoil in longitudinal turbulence, *Journal of Aircraft* 34 (5) (1997) 619–626.
[37] D.C. Poirel, S.J. Price, Structurally nonlinear fluttering airfoil in turbulent flow, *AIAA Journal* 39 (10) (2001) 1960–1968.
[38] J.N. Newman, *Marine Hydrodynamics*, MIT Press, Cambridge, 1978.